HHS Public Access

Author manuscript

Photochem Photobiol Sci. Author manuscript; available in PMC 2019 November 01.

Published in final edited form as:

Photochem Photobiol Sci. 2018 November 01; 17(11): 1515–1533. doi:10.1039/c8pp00195b.

Fullerenes as Photosensitizers in Photodynamic Therapy: Pros and Cons

Michael R Hamblin*

Wellman Center for Photomedicine, Massachusetts General Hospital, Boston, MA 02114, USA; Department of Dermatology, Harvard Medical School, Boston, MA 02115, USA; Harvard-MIT Division of Health Sciences and Technology, Cambridge, MA 02139, USA

Abstract

One class of carbon nanomaterials is the closed cages known as fullerenes. The first member to be discovered in 1985 was C60, called “buckminsterfullerene” as its cage structure resembled a geodesic dome. Due to their extended π-conjugation they absorb visible light, possess a high triplet yield and can generate reactive oxygen species upon illumination, suggesting a possible role of fullerenes in photodynamic therapy (PDT). Pristine C60 is highly hydrophobic and prone to aggregation, necessitating functionalization to provide aqueous solubility and biocompatibility. The most common functional groups attached are anionic (carboxylic or sulfonic acids) or cationic (various quaternary ammonium groups). Depending on the functionalization, these fullerenes can be designed to be taken up into cancer cells, or to bind to microbial cells (Gram-positive, Gram-negative bacteria, fungi). Fullerenes can be excited with a wide range of wavelengths, UVA, blue, green or white light. We have reported a series of functionalized fullerenes (C60, C70, C82) with attached polycationic chains and additional light-harvesting antennae that can be used in vitro and in animal models of localized infections. Advantages of fullerenes as photosensitizers are: (a) versatile functionalization; (b) light-harvesting antennae; (c) ability to undergo Type 1, 2, and 3 photochemistry; (d) electron transfer can lead to oxygen-independent photokilling; (e) antimicrobial activity can be potentiated by inorganic salts; (f) can self-assemble into supramolecular fullerosomes; (g) components of theranostic nanoparticles; (h) high resistance to photobleaching. Disadvantages include: (a) highly hydrophobic and prone to aggregation; (b) overall short wavelength absorption; (c) relatively high molecular weight; (d) paradoxically can be anti-oxidants; (e) lack of fluorescence emission for imaging.

Graphical Abstract

Fullerenes can act as photosensitizers for photodynamic therapy. Advantages include chemical and photochemical versatility, nanotechnology potential, resistance to photobleaching. Disadvantages include short wavelength absorption, pronounced aggregate and high molecular weight.

* Hamblin@helix.mgh.harvard.edu.

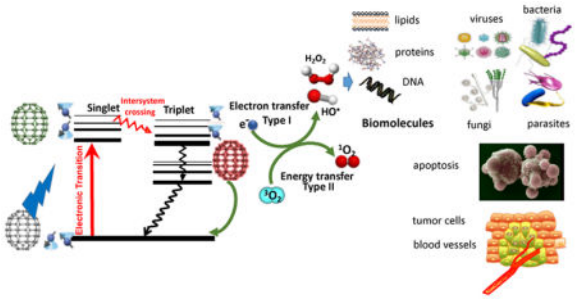

Keywords

photodynamic therapy; antimicrobial photodynamic inactivation; photochemical pathways; fullerenes; polycationic chains; light-harvesting antennae; localized infections

1. Introduction

Eiji Osawa of Toyohashi University of Technology in Japan, predicted the existence of C60 in 1970 [1]. He realized that the structure of a corannulene molecule could be viewed as an isolated part of a soccer ball, and hypothesized that the complete spherical structure could also exist as a stable molecule. Also in 1970, R. W. Henson who was a member of the Graphite and Carbon Studies Group at the Atomic Energy Research Establishment, Harwell, UK independently proposed the soccer ball structure and created a model of C60 [2]. The results were never published but were acknowledged in Carbon in 1999 [3]. In 1973 a group of scientists from the USSR made a quantum-chemistry analysis of the stability of C60 and calculated its electronic structure. The paper was published in 1973 in the Proceedings of the USSR Academy of Sciences (in Russian) [4]. Fifteen years later, in 1985 Harold Kroto of the University of Sussex, UK, visited Robert Curl and Richard Smalley at Rice University, TX, to test whether their high-power laser apparatus could simulate the surface of a carbon-rich “red giant” star. They discovered C60 as a peak in the mass spectrum, and this work eventually led to the award of the 1996 Nobel Prize in Chemistry [5].

The structure of the most common fullerene (C60) is a truncated icosahedron composed of twenty hexagons and twelve pentagons (Figure 1). The next most common fullerene is C70 which is more ovoid in shape, rather than entirely spherical [32]. Other fullerenes with 72, 76, 84 and even 108 carbon atoms have been prepared [6]. Since the original discovery there has been intense interest in researching possible biological applications of fullerenes (and other carbon nanostructures produced in the nanotechnology revolution) with a view to using fullerenes in medicine [7–9].

Photodynamic therapy (PDT) was discovered over 100 years ago in 1900 in Munich, Germany. by a medical student called Oscar Raab who was working with Prof Hermann von Tappenier. He observed that when the single-cell microorganisms called paramecia were incubated with the fluorescent dye, acridine orange and exposed to light, they were killed, while those kept in the dark survived [10]. When it was soon discovered that this phenomenon required oxygen to be present, the term “photodynamic” was coined [11]. It was realized in

1910 that this photodynamic effect could be used as a medical therapy (photodynamic therapy or PDT) to destroy undesirable biological tissue, such as skin cancers [12].

The photochemical mechanism of PDT was first reported in 1977 by Weishaupt et al [13]. They identified singlet molecular oxygen as the most important cytotoxic agent in the destruction of cancer cells incubated with hematoporphyrin and exposed to red light. It was later realized that the key feature of compounds (dyes) such as porphyrins used for PDT, was the existence of a long-lived triplet state that could be formed by an "intersystem crossing process" from the excited singlet state porphyrin, formed when the ground state porphyrin absorbed a photon of energy [14]. Since ground state oxygen has a triplet electronic configuration, the excited porphyrin triplet state is allowed to undergo energy transfer with oxygen to produce the ground state singlet porphyrin and the excited state singlet oxygen ($^1O_2$). $^1O_2$ is a highly reactive molecule that can oxidize lipids, proteins and nucleic acids, thus causing the death of any kind of cells (bacteria, fungus, cancer, normal cells, etc). Because $^1O_2$ is highly reactive, it can only damage tissue or cells in the precise location where it is produced (i.e. where both dye and light are present at the same time).

In addition to $^1O_2$, (which became known as the Type II photochemical mechanism), it was realized that other different reactive oxygen species (ROS) were also involved in the PDT effect depending on a number of factors. These ROS (including hydroxyl radicals, hydrogen peroxide, and superoxide anion) were produced by what became known as the Type I photochemical mechanism [15]. It is thought that this process initially involves a 1-electron transfer from the PS triplet state to oxygen to form superoxide anion. Two additional 1-electron reduction steps may then transform superoxide into hydrogen peroxide and then to hydroxyl radicals [16]. The two photochemical mechanisms (Type 1 and Type 2) are schematically shown in a Jablonski diagram in Figure 2. These highly reactive oxygen species (ROS) $^1O_2$ and $HO^{\bullet}$ can cause oxidative damage to damage to nucleic acids, lipids and proteins and effectively kill cancer cells or even normal cells, and destroy any type of microorganisms whether they are Gram-positive bacteria, Gram-negative bacteria, fungi, viruses or parasites [17].

The goal of the present review is to discuss some of the papers published from the Hamblin laboratory in the Wellman Center for Photomedicine at Massachusetts General Hospital that have looked at PDT mediated by fullerenes [18]. The goal is not to present a comprehensive review of fullerene-based PDT; the field has now grown far beyond that which can be fully covered in a single review. Moreover, we have concentrated to a large extent (but not exclusively) on antimicrobial photodynamic inactivation, and have expended less effort discussing anti-cancer applications and in vitro PDT of cancer cells. Nevertheless, our studies have uncovered some useful pieces of information that would not be immediately obvious to someone starting to work in this field. Our summary of the pros and cons of fullerenes as photosensitizers in PDT will likely be useful to other investigators.

2. Photochemical mechanisms

It has been known since shortly after the discovery of fullerenes that they could catalyze the formation of ROS after illumination of both pristine and functionalized C_{60} [19]. In a similar

manner to the tetrapyrrole-based PS discussed above [20, 21], illumination of fullerenes dissolved in organic solvents in the presence of oxygen leads to the efficient generation of $^1O_2$ via energy transfer from the excited triplet state of the fullerene [22]. However, in polar solvents, especially those containing reducing agents (such as NADH at concentrations found in cells), illumination of various fullerenes will generate different kinds of ROS, such as superoxide anion [23]. These two pathways (singlet oxygen and superoxide anion) are analogous to the Type II and Type I photochemical mechanisms discussed in PDT [14, 24].

Fullerenes with their triply degenerate, low lying lowest unoccupied molecular orbitals (LUMO) are excellent electron acceptors capable of accepting as many as six electrons [25]. There is some evidence that fullerene excited states (in particular the triplet) are even better electron acceptors than the ground state [26, 27]. It is thought that the reduced fullerene triplet or radical anion can transfer an electron to molecular oxygen forming superoxide anion radical $O_2^{-\bullet}$.

Yamakoshi et al [23] carried out a photochemical study comparing energy transfer processes (singlet oxygen $^1O_2$) and electron transfer (reduced active oxygen radicals such as superoxide anion radical $O_2^{-\bullet}$), using various scavengers of ROS, physicochemical (electron paramagnetic resonance (EPR) radical trapping and near-infrared spectrometry), and chemical methods (nitro blue tetrazolium reaction with superoxide). Whereas $^1O_2$ was generated effectively by photoexcited C_{60} in nonpolar solvents such as benzene and benzonitrile, they found that $O_2^{-\bullet}$ and $HO^{\bullet}$ were produced instead of $^1O_2$ in polar solvents such as water, especially in the presence of a physiological concentration of reductants including NADH.

Miyata et al solubilized fullerenes into water with polyvinylpyrrolidone (PVP) as a detergent [28]. Visible-light irradiation of PVP-solubilized C_{60} in water in the presence of NADH as a reductant and molecular oxygen resulted in the formation of $O_2^{-\bullet}$, which was detected by EPR spin-trapping. Formation of $O_2^{-\bullet}$ was also evidenced by the direct observation of a characteristic signal of $O_2^{-\bullet}$. On the other hand, no formation of $^1O_2$ was observed using TEMP as a $^1O_2$ trapping agent. Likewise, no near-IR luminescence (1270 nm) of $^1O_2$ was observed. These results suggest that the PDT activity of the PVP-solubilized fullerene was caused not by $^1O_2$, but by reduced oxygen species such as $O_2^{-\bullet}$, which were generated by the electron-transfer reaction of $C_{60}^{-\bullet}$ with molecular oxygen.

One potentially confusing and paradoxical aspect of light-activated fullerenes, is how can these compounds behave as powerful anti-oxidants in the dark, and powerful PDT agents when illuminated? The fact that fullerenes are indeed powerful anti-oxidants is beyond dispute [29]. One clue that might explain this inconsistency was proposed in 2009, by Andrievsky et al. [30], who showed that one major mechanism to explain how hydrated C60 can inactivate the highly reactive ROS, hydroxyl radical, not by covalently scavenging the radicals, but rather by action of the coat of “ordered water” that was linked to the fullerene nanoparticle [31]. One of the explanations is that hydroxyl radicals can be slowed down or trapped for a sufficient time allowing the two radicals to react with each other, which produce the comparatively less-toxic ROS, hydrogen peroxide.

3 Synthetic modification of fullerenes for PDT

The two most important reactions to allow the covalent functionalization of fullerenes are the Bingel reaction and the Prato reaction (shown in Figure 3). The Bingel reaction is a cyclopropanation reaction onto a fullerene to produce a methanofullerene. This reaction was first discovered by C. Bingel in 1993 using the bromo-derivative of diethyl malonate in the presence of a base such as sodium hydride or DBU [32]. This reaction prefers to take place at the shorter of the two types of double bonds on the fullerene surface; i.e. at the junctions of two hexagons (6–6 bonds) and the driving force is the relief of steric strain. The Prato reaction is a particular example of the well-known 1,3-dipolar cycloaddition of azomethine ylides to double bonds to produce 5-membered rings such as pyrrolidines [33]. In fullerenes for instance, the amino acid sarcosine reacts with paraformaldehyde when heated at reflux in toluene to give an ylide which reacts with a double bond in the 6,6 ring position via a 1,3-dipolar cycloaddition to yield a N-methylpyrrolidine fullerene derivative in 82% yield [34].

A highly water-soluble hexa(sulfobutyl)fullerene (FC4S) was synthesized by the treatment of C_{60} in dimethoxyethane with sodium naphthalide followed by reacting the resulting hexa-anionic fullerene intermediate with an excess of 1,4-butanesulfone [35] as shown in Figure 4. Direct detection of $^1O_2$ production from FC4S self-assembled nanospheres after irradiation at 500–600 nm was obtained by the measurement of its near-infrared luminescence at 1270 nm. Despite FC4S having a relatively low optical absorption at 600 nm, an appreciable $^1O_2$ signal was detected comparable to that of Photofrin at the same molar concentration, but less than sulfonated aluminium phthalocyanine, AlS_4Pc. The quantum yield of FC4S for the generation of $^1O_2$ in H_2O was estimated to be 0.36 using a correlation with C_{60} encapsulated in γ-cyclodextrin. Chiang and his coworkers showed that FC4S spontaneously self-assembled into hexameric hydrophilic nanospheres [35] (Fig 4).

It is known that cationic functional groups provide good solubility to otherwise hydrophobic molecules, and moreover have the potential to bind to the anionic residues overexpressed on cancer cells and on bacterial cell walls via static charge interactions. Therefore, cationic groups have been considered a good choice for attachment to the fullerene cage to prepare PS. A number of chemical functionalization techniques for fullerenes have been evaluated [36, 37]. Among them, general suitable methods for the preparation of cationic fullerene derivatives include cyclopropanation (Bingel reaction) [38] eg $C_{60}[>M(C_3N_6{}^+C_3)_2]\text{-}(I^-)_{10}$ (LC14, Figure 5) [39, 40] and $C_{70}[>M(C_3N_6{}^+C_3)_2]\text{-}(I^-)_{10}$ (LC17, Figure 6) [41]. Pyrrolidination [42] eg quaternized dimethylpyrrolidinium [43] fullerenyl monoadduct (BB4, Figure 7) and trisadduct (BB6, Figure 7) and structures such as LC22 and LC24 [44, 45].

Throughout this review we have retained the compound numbers that were used in the original publications to avoid any confusion.

The cyclopropanation reaction of C_{60} was applied recently for the attachment of a highly complex decacationic moiety to the fullerene cage leading to the formation of fullerenes bearing ten positive charges. The decacationic functional derivatives of C_{60}, C_{70}, and $C_{84}O_2$ fullerenes were designed to increase both the water-solubility and provide surface binding interactions with –*D*-Ala-*D*-Ala residues of the bacteria cell wall by incorporating multiple

H-bonding interactions and positive quaternary ammonium charge to bind to anionic lipopolysaccharides and lipoteichoic acids. The design included two esters and two amide moieties to give a sufficient number of carbonyl and –NH groups in a short length of ~20 Å to provide effective multi-binding sites with the use of a well-defined water-soluble pentacationic moiety $C_3N_6^+C_3$-OH at each side of the arm. A similar reaction scheme using a malonate precursor arm $M(C_3N_6C_3)_2$ was also applied for the preparation of $C_{84}O_2[>M(C_3N_6^+C_3)_2]$ $(I^-)_{10}$ (LC19), $C_{84}O_2[>M(C_3N_6^+C_3)_2][>M(C_3N_6C_3)_2]$ (LC20), $C_{70}[>M(C_3N_6^+C_3)_2][>M(C_3N_6C_3)_2]$ (LC18) [40] (Figure 6).

To circumvent the shortcoming of weak absorption of visible light wavelength by fullerenes, a highly fluorescent donor chromophore antenna can be covalently attached to fullerenes. Dialkyldiphenylaminofluorene (DPAF-Cn, shown in Figure 5) can function as a light-harvesting donor chromophore antenna that can be attached to C60 cage to facilitate ultrafast intramolecular energy- and electron-transfer from the donor antenna to C60 and therefore to enhance PDT efficacy [46].

It was reported the majority of the HOMO electron density was delocalized over the dialkyldiphenylaminofluorene (DPAF-C_n) moiety, whereas the LUMO electron density was located on the C_{60} spheroid [47]. Therefore charge-separated states may be generated by intramolecular electron-transfer between the diphenylaminofluorene donor and C_{60}> acceptor moieties during the photoexcitation process.

Intramolecular formation of transient charge-separated states is crucial for generation of radical ROS, initially with $O_2^{-\bullet}$ and subsequently $HO^{\bullet}$. $^1C_{60}^{-*}\bullet(>CPAF^{+\bullet}\text{-}C_n)$ is the most stable charge-separated state in polar solvents, including H_2O [47] and has nearly 6-fold higher generation of singlet O_2 compared to $^1C_{60}^{-*}\bullet(>DPAF^{+\bullet}\text{-}C_n)$.

Many strategies have been applied to either solubilize or modify fullerenes in order to avoid the problem of aggregation, and to thereby improve their drug-delivery and suitability for medical use: *e.g.* liposomes, [48–50], micelles [51, 52], dendrimers [53, 54], PEGylation [54–57], self-nanoemulsifying systems (SNES) [58–61] and encapsulation in cyclodextrins [48, 62, 63].

4 Fullerene-mediated PDT for cancer: in vitro studies

Many studies of fullerenes for PDT have used them as PS to combat cancer. PDT began to be widely studied in the 1970s as a clinical anticancer treatment [64–66]. The first step in PDT anticancer investigation has traditionally been to test if the combination of fullerenes and visible light could kill cancer cells in cell culture experiments in vitro

It is considered that one condition for any PS to produce cell killing after illumination, is that the PS should actually be taken up inside the cell, as the production of ROS outside the cell will not be enough to produce cell death, unless it is produced in extremely large amounts. One of the limitations for the study of the uptake of fullerenes into cells is their non-fluorescent nature that limits the use of fluorescence microscopy to study the localization in cells. Some strategies though have been adopted to overcome this limitation, such as the use of radiolabeled fullerene that have been prepared to study the uptake. Indirect immunofluorescence staining with antibodies has been used to show the localization

of fullerene in mitochondria and other intracellular membranes [67]. Recently energy-filtered transmission electron microscopy and electron tomography was used to visualize the cellular uptake of pristine C_{60} nanoparticulate clusters in the plasma membrane, lysosomes and in the nucleus of cells [68].

The first report of phototoxicity in cancer cells mediated by fullerenes was in the year 1993. In this study Tokuyama et al [69] used carboxylic acid functionalized fullerenes at 6.0 μM and white light to produce growth inhibition in cancer cells. Burlaka et al [70] used pristine C_{60} at 10 μM with visible light from a mercury lamp to produce some phototoxicity in Ehrlich carcinoma cells or in rat thymocytes. The cytotoxic and photocytotoxic effects of two water-soluble fullerene derivatives, a dendritic C_{60} mono-adduct and the malonic acid C_{60} trisadduct were tested on Jurkat cells when irradiated with UVA or UVB light [69]. The cell death was mainly caused by membrane damage and it was UV dose-dependent. Three C_{60} derivatives with two to four malonic acid groups (DMA C_{60}, TMA C_{60} and QMA C_{60}) were tested for their relative efficacy in HeLa cells and the results showed the following order for their efficacy DMA C_{60} >TMA C_{60} > QMA C_{60} [69].

The hypothesis that fullerenes have the potential to destroy cancer cells by PDT was tested in our group. We showed that the C_{60} molecule mono-substituted with a single pyrrolidinium group (BB4 shown in Figure 7) is an efficient PS, and can mediate killing of a panel of mouse cancer cells. The mouse cells that we used were lung cancer (LLC), colon adenocarcinoma (CT26) and reticulum cell sarcoma (J774), and the latter showed much higher susceptibility to fullerene mediated PDT possibly due to having an increased uptake (because J774 cells behave like macrophages) [71]. Besides the exceptionally active BB4, the next group of compounds had only moderate activity against J774 cells showing only some killing even at high fluences. The indirect measurement of fullerenes uptake was demonstrated by increase in fluorescence of an intracellular probe (H_2DCFDA) which is specific for the formation of ROS. We also showed the initiation of apoptosis by PDT mediated by BB4 and BB6 in CT26 cells at 4–6 h after illumination. The induction of apoptosis was rapid after illumination which may perhaps suggest that fullerenes are localized in mitochondria, as it has been previously shown with benzoporphyrin derivative [72–74].

The explanation for the mono-pyrrolidinium substituted fullerene as most effective PS most likely linked to its relative hydrophobicity as established by its logP value of over 2. Besides this a single cationic charge on BB4 is in addition expected to play a significant role in determining its relative phototoxicity. On comparing the effectiveness of BB4 to Photofrin® [57] we found that BB4 was far better at PDT-mediated killing of human ovarian cancer cells *in vitro* than Photofrin. Both showed a light-dose dependent response. Though, the response of BB4 at the light fluences used was much more pronounced than that of Photofrin, demonstrating that BB4 was a considerably superior photosensitizer than Photofrin against ovarian cancer cells *in vitro*.

As fullerenes show a relatively slower uptake we incubated the cells for 24h with $C_{70}[>M(C_3N_6^+C_3)_2]$ LC14 (Figure 5) and $C_{60}[>M(C_3N_6^+C_3)_2]$ LC17 (shown in Figure 6). $C_{70}[>M(C_3N_6^+C_3)_2]$ killed cells more effectively than $C_{60}[>M(C_3N_6^+C_3)_2]$, On the

contrary, the fullerene LC14 killed less than 1 log at all fluences. LC-17 that was without the decatertiary amine chain was less phototoxic than LC18 which possessed an extra deca-tertiary ethyleneamine chain. This exciting result prompted us to carry out studies with new PDT compounds $C_{84}O_2[>M(C_3N_6^+C_3)_2]$-$(I_3^-)_{10}$ (LC19-I_3^-) and $C_{84}O_2[>M(C_3N_6^+C_3)_2][>M(C_3N_6C_3)_2]$-$(I^-)_{10}$ (LC20) (shown in Figure 6). Different wavelengths were used for irradiation. UVA and blue light caused more killing with LC20 than with LC19-I_3^-. This difference can be attributed to a higher chance of an electron transfer process occurring with shorter wavelengths and also the presence of the electron donating tertiary-ethyleneamine chain. When white light was employed, the variation between LC20 and LC19-$I_3^-$was smaller, but LC20 still gave extra killing. When green light was used, there was equal killing for both fullerenes. When red light was used the situation was reversed and LC19-I_3^-gave considerably more killing than LC20. It is important to state that all the compounds induced very low dark toxicity [56].

5 Fullerene-PDT for cancer: in vivo studies

The three prerequisites for a fullerene PS to have an important PDT effect on tumors are first of all it should accumulate in the tumor tissue; secondly there should be an efficient way to administer the compound to tumor bearing animals; and thirdly a practical way to deliver excitation light to the tumors. The first effort in this direction was reported by Tabata [35] in 1997. To render the normally water-insoluble pristine C_{60} water-soluble, and enlarge its molecular size they chemically modified it with polyethylene glycol. This conjugate was injected intravenously into mice carrying a subcutaneous tumor on the back. C_{60}-PEG conjugate demonstrated higher accumulation and relatively more prolonged retention in the tumor tissue than in normal tissue. On performing PDT after intravenous injection of C_{60}-PEG conjugate or Photofrin to tumor-bearing mice, coupled with exposure of the tumor site to visible light, the volume increase of the tumor mass was suppressed and the C_{60}-PEG conjugate exhibited a stronger suppressive effect than Photofrin. Tumor necrosis was observed without any damage to the overlying normal skin. The antitumor effect of the conjugate showed an increase with increasing fluence delivered and C_{60} dose, and cures were achieved by treatment with a low dose of 424 μg/kg at a fluence of 107 J/cm^2. In another study Liu and others [7576] conjugated polyethylene glycol (PEG) to C_{60} (C_{60}-PEG), and diethylenetriaminepentaacetic acid (DTPA) was subsequently introduced to the terminal group of PEG to prepare C_{60}-PEG-DTPA that was mixed with gadolinium acetate solution to obtain Gd^{3+}-chelated C_{60}-PEG-DTPA-Gd. PDT induced anti-tumor effect and MRI tumor imaging was evaluated on intravenous injection of C_{60}-PEG-DTPA-Gd into the tumor bearing mice. Equivalent generation of superoxide upon illumination was observed with or without Gd^{3+} chelation. Intravenous injection of C_{60}-PEG-DTPA-Gd into tumor bearing mice plus light (400~500 nm, 53.5 J/cm^2) demonstrated significant anti-tumor PDT depending on the timing of light irradiation that also correlated with tumor accumulation as detected by the enhanced MRI signal.

Chiang and his coworkers [75] performed a preliminary *in vivo* study of PDT using hydrophilic nanospheres formed from hexa(sulfo-*n*-butyl)-C_{60} (FC_4S, shown in Figure 4). This study was performed on ICR mice bearing sarcoma 180 subcutaneous tumors. No adverse effects were noted in the animals when the FC_4S was administered orally. Water-

soluble FC_4S in PBS (5 mg/kg body weight) was given either intraperitoneally or intravenously with subsequent irradiation with an argon ion laser beam at a wavelength of 515 nm or an argon-pumped dye-laser at 633 nm. The beam was focused to a diameter of 7–8 mm with the total light dose of 100 J/cm^2. Inhibition of tumor growth was found more effective using the low wavelength i.e. in case of better-absorbed 515nm laser than the 633-nm laser. *I.p.* administration method proved to be slightly better in inhibition effectiveness than the *i.v.* method. Conclusively data suggest that PDT with fullerenes is not only possible in animal tumor models, but can demonstrate the potential use of these compounds as PS for PDT of cancer.

We also demonstrated [77] the therapeutic effects of intraperitoneal PDT with a fullerene excited by white light in a very challenging mouse model of disseminated abdominal cancer. In this study we formulated the monocationic BB4 (Figure 7) in micelles composed of Cremophor EL. Colon adenocarcinoma cell line (CT26) expressing firefly luciferase was used to allow monitoring of IP tumor burden by non-invasive bioluminescence imaging. BB4 in micelles was injected intraperitonally (5 mg/kg) followed by white-light illumination (100 J/cm^2) delivered through the peritoneal wall. To facilitate this unusual approach, the skin overlying the peritoneal wall was temporarily peeled back to allow light penetration and sutured up again afterwards. The mice recovered from this surgical procedure without any problem. This treatment produced a statistically significant reduction in bioluminescence and a survival advantage in mice, shown in Figure 4. A drug-light interval of 24 hours was more effective than a 3-hour drug-light interval showing the significance of allowing enough time for the fullerene to be taken up into the cancer cells in the peritoneal cavity.

As the cancer cells are known to express more glucose receptors, Otake and el. exploited this fact and synthesized C_{60}-glucose conjugates which also proved to be more soluble. These conjugates demonstrated selective phototoxicity in cancer cells compared to fibroblast cells thus suggesting the importance of targeting glucose receptors [78]. The PDT effect *in vivo* was investigated in human-melanoma (COLO679)-xenograft bearing mice by injecting C_{60}-$(Glc)_1$ (0.1 or 0.2 mg/tumor) intratumorally followed by irradiation with 10 J/cm^2 UVA1. The drug-light interval was 4h. Tumor growth was suppressed better with the higher dose than the lower dose.

6 Fullerene-PDT for infections: in vitro studies

Antibiotic resistance is a worldwide problem that is spreading with remarkable speed [79]. The injudicious and over-use of antibiotics is the most important reason leading to antibiotic resistance around the world. The “golden age” of antimicrobial therapy began with the discovery of antibiotics around the middle of the last century [80]. Meanwhile, many other well-established effective treatments that could kill bacteria and cure infections (including photosensitizing reactions) were forgotten. In the last few decades, however, concerns have emerged about the re-ermergence of “untreatable infections” caused by “superbugs” [81, 82]. These concerns have created an ever-increasing need and demand for new antibiotic drugs. However new antibiotics are simply not being discovered at the requisite rate [83, 84], motivating the investigation of antimicrobial photodynamic inactivation (aPDI) [17] as a new alternative approach.

As a result of these pressures, antimicrobial PDT or aPDI has become an emerging alternative strategy to destroy microorganisms especially for multi-drug resistant pathogens [85]. PDT produces ROS that are toxic to the target microorganisms. PDT has a broad spectrum of action, and compared to antibiotic treatment, PDT does not lead to the selection of mutant resistant strains.

Currently, topical application of the PS solution onto or into the infected tissue, and subsequent illumination with activating light seems to be the most appropriate method to carry out antimicrobial PDT, without damaging the surrounding tissue or disturbing the residual bacterial-flora. Since the infecting microbial cells are often confined to the surface layers of the tissue, and the PS distribution is perforce fairly superficial, it does not appear to be highly detrimental if the penetration of the light is also only superficial, as might be the case for the UVA or blue light used to excite fullerenes. It has been well accepted that Gram-positive bacteria are more susceptible to PDT as compared to Gram-negative bacteria. This can be explained by the different structures of their cell walls [86].

There are several possible mechanisms to explain the antimicrobial activity of illuminated fullerene PS: by interfering with cell wall synthesis; plasma membrane integrity; nucleic acid synthesis; ribosomal function and folate synthesis. All of these processes would result in disruption of the bacterial cell structure and metabolism and complete inhibition of growth. Martin and Logsdon hypothesized that it was possible that microorganisms were susceptible to damage by to Type I ROS when compared with Type II singlet oxygen [87]. As mentioned before, the solubility of fullerenes is improved by functionalization [36] and when hydrophilic or amphiphilic functional groups [88] are attached to the fullerenes light activation will more efficiently produce hydroxyl radicals and superoxide anion (as well as singlet oxygen) [89].

An ideal PS proposed for antimicrobial PDT can be judged on several criteria. These PS should have no toxicity in the dark and should selectively kill bacteria over mammalian cells. PS should be able to kill multiple classes of microorganisms at relatively low concentrations with low fluences of light. PS should ideally have high absorption coefficients between 600 nm to 800 nm where the penetration of light into tissue is highest, and have high quantum yields of both triplet state and singlet oxygen formation.

The structures, especially the charges of the groups attached to the fullerenes influences the efficacy of photokilling of microorganisms. Our lab has shown, in a series of reported experiments that cationic fullerenes fulfill many, but not all of the aforementioned criteria. For the first time we demonstrated that the soluble functionalized fullerenes were efficient antimicrobial PS and could mediate selective photodynamic inactivation (PDI) for various classes of microbial cells over mammalian cells [90]. We compared the antimicrobial activity of broad-spectrum antimicrobial photodynamic activities of two series of functionalized C_{60}; a first series with one, two, or three polar diserinol groups (BB1–3), and a second series with one, two, or three quarternary pyrrolidinium groups (BB4–6). Gram-positive bacteria (*S. aureus*) Gram-negative bacteria (*E. coli* and *P. aeruginosa*), and fungal yeast (*C. albicans*) were tested in this study. The neutral, alcohol-functionalized fullerenes (BB1–3) had only modest activity against *S. aureus*, while the cationic pyrrolidinium-functionalized fullerenes

(BB5 and 6) were surprisingly effective in causing light-mediated killing of *S. aureus* at 1uM, and 10uM for *E. coli*, *C. albicans* and *P. aeruginosa.* However, these pyrrolidinium-functionalized fullerenes compounds (especially BB5 and BB6) demonstrated high levels of dark toxicity against *S. aureus*, as Mashino et al. showed that cationic fullerenes could inhibit the growth of *E. coli* and *S. aureus* by interfering with the respiratory chain [91, 92]. These compounds all performed significantly better than a widely used antimicrobial photosensitizer, toluidine blue O.

In agreement with previous findings, results from Spesia et al. [93] indicated that a dicationic fullerene derivate was an interesting PDT agent with potential applications in PDI of bacteria. They compared PDI efficacy of fullerene derivatives with different numbers of cationic charged. The spectroscopic and photodynamic properties of a dicationic *N,N*-dimethyl-2-(40-*N,N,N*-trimethylaminophenyl) fulleropyrrolidinium iodide) (DTC_{60}^{2+}) were compared with a non-charged *N*-methyl-2-(4′-acetamidophenyl)fulleropyrrolidine (MAC_{60}) and a monocationic *N,N*-dimethyl-2-(4′-acetamidophenyl)fulleropyrrolidinium iodide (DAC_{60}^{+}) in different media and in a typical Gram-negative bacterium, *E. coli*. PDI of *E. coli* cellular suspensions by dicationic fullerene exhibits a ~3.5 log decrease of cell survival after 30 min of irradiation, which represents about 99.97% of cellular inactivation.

To determine the optimal chemical structure of the fullerene derivatization, a QSAR relationships study employed fullerene PS with a wider range of different hydrophobicities, as well as an increased number of cationic charges [94]. The results indicated that increasing the number of cationic charges and lowering the hydrophobicity tended to increase the antimicrobial PDI efficacy of fullerene PS against both Gram-positive and Gram-negative bacteria. The charge increases the association of the PS with negatively charged pathogen membranes, whereas the hydrophobic character increases association with or penetration into the lipid components of the membrane, or both. Mizuno et al. [43] from our laboratory emphasized the importance of the number of cationic charges in influencing the efficiency of the fullerenes in antimicrobial PDI when they looked at a further series of functionalized cationic fullerenes PS. They compared PDI efficacy of a new group of synthetic fullerene derivatives that possessed either basic or quaternary amino groups as antimicrobial PS against *S aureus* (Gram-positive), *E. coli* (Gram-negative) bacteria and *C. albicans* (fungi). QSAR derived with LogP and hydrophilic lipophilic balance parameters showed that much better correlations were obtained when 3X the number of cationic charges were subtracted from the LogP values. The most effective ones to perform antimicrobial PDT were tetracationic compound BB21 that had more cationic charges and a lower logP. *S. aureus* was most susceptible; *E. coli* was intermediate, while *C. albicans* was the most resistant species tested.

The antimicrobial effects of two highly water-soluble decacationic fullerenes LC14 ($C_{60}[>M(C_3N_6^{+}C_3)_2]$) and LC17 ($C_{70}[>M(C_3N_6^{+}C_3)_2]$) were compared in the PDT-killing of the Gram-positive *S. aureus* [39]. The decacationic arms attached to these fullerenes allowed the rapid binding to the anionic residues of bacterial cell walls. The large number of ionic groups dramatically enhanced the water solubility of these compounds. The data showed interesting differences between the photoactivity of the decacationic fullerene compounds that differed only in the number of carbon atoms in the fullerene cage. For

Gram-positive bacteria LC14 was better at photokilling than LC17, while for Gram-negative bacteria and for cancer cells the opposite was the case. The results of ROS ($HO^{\bullet}$ or $^1O_2$) generation demonstrated that LC14 produced more $^1O_2$ while LC17 produced more HO•. This finding offers an explanation of the preferential killing of Gram-positive bacteria by LC14 and the preferential killing of Gram-negative bacteria by LC17. This finding is in agreement with our previous report that Type-II ROS, i.e. singlet oxygen, $^1O_2$, are better at killing Gram-positive bacteria than Type-I ROS, i.e. hydroxyl radicals, HO•, while the reverse is true for Gram-negative bacteria (HO• is better at killing than $^1O_2$). The hypothesis is that $^1O_2$ can diffuse more easily into porous cell walls of Gram-positive bacteria to reach sensitive sites, while the less permeable Gram-negative bacterial cell wall needs the more reactive HO• to cause real damage [95, 96].

The addition of azide can be used to distinguish between Type 1 and Type 2 photochemical mechanisms [97]. This is because azide quenches singlet oxygen by both physical and chemical quenching processes and tends to reduce microbial killing where the mechanism is largely Type 2 in nature. However in some cases the addition of azide can actually increase the microbial killing, so-called “paradoxical potentiation” [98]. The phenothiazinium dye, methylene blue was the first to be shown to be potentiated by azide [99], and then we subsequently showed that some other phenothizinium PS could also be potentiated by azide [100]. We explored the effects of azide on PDI mediated by three different fullerene PS, LC14, LC15 and LC16 (Figure (C60[>M(C3N6(+)C3)2][>M(C3N6C3)2]-(I(-))10 (LC16 was derived from LC14), as a malonate bisadduct containing a covalently bound decatertiary amine arm [101]. Bacterial killing was not much inhibited by addition of azide anions, and in some cases was potentiated. In the absence of oxygen, microbial photokilling was highly potentiated (up to 5 logs) by the addition of azide anions. Oxygen-independent bacterial photokilling was probably mediated by azidyl radicals formed by a 1-electron transfer process.

7 Fullerene-PDT for infections: in vivo studies

The absorption spectrum of fullerenes is, in addition to substantial UV absorption, mainly in the blue and green visible wavelengths. This property actually limits the application of fullerene in clinical disorders, since the penetration of short wavelength light into tissue is relatively poor; however, fullerenes may still be useful as antimicrobial PS for the treatment of relatively superficial infections, where the light does not need to penetrate deeper than 1mm. A fullerene-based PS (BB6) with tricationic charges provided by quaternized dimethylpyrrolidinium groups was found to be an effective against Gram-positive bacteria, Gram-negative bacteria and fungal yeast *in vitro* [102]. To investigate if the high degree of *in vitro* activity could translate into an *in vivo* antibacterial PDT effect, our lab [42] continued to test BB6 in two potentially lethal mouse models of wounds infected with two Gram-negative bacteria (*P. aeruginosa* and *P. mirabilis),* respectively. Compared to Gram-positive bacteria, many Gram-negative bacteria are much more difficult to be photo-inactivated, and tend to produce systemic sepsis when wound infections develop. Higher concentrations of PS and higher fluences of light (180 J/cm^2) were needed *in vivo* than *in vitro* to achieve a certain loss of bioluminescence. The fullerene-mediated PDT succeeded in saving the life of mice whose wounds were infected with *P. mirabilis* and could be combined with a sub-optimal

dose of antibiotics to save mice with *P. aeruginosa* wound infections. These results shown in Figure 9 indicated that fullerene-mediated PDT could either treat wounds infected with virulent species of Gram-negative bacteria or be able to synergize with a suboptimal antibiotic regimen to prevent regrowth and produce significantly higher survival [42].

In the case of 3rd-degree burns, they are particularly susceptible to bacterial infection as the barrier function of the skin is destroyed, the dead tissue is devoid of host-defense elements, and a systemic immune suppression is a worrying consequence of serious burns. Furthermore the lack of perfusion of the burned tissue means that systemic antibiotics are generally ineffective [103]. Although excision and skin grafting is now standard treatment for 3rd-degree burns [104], superimposed infection is still a major problem. Patients with Gram-negative burn infections have a higher likelihood of developing sepsis than Gram-positive infections. Topical antimicrobials are the mainstay of therapy for burn infections and PDT may have a major role to play in the management of this disease [94].

We found in previous study a decacationic fullerene LC17 (C_{70}[>M($C_3N_6{}^+C_3)_2$]) was good at photokilling Gram-negative bacteria *in vitro*. We synthesized a new compound C_{70}[>M($C_3N_6{}^+C_3)_2$][>M($C_3N_6C_3)_2$] (LC18) with the same decacationic side chain plus an additional deca tertiary amine groups against Gram-negative bacteria (Figure 6). A mouse model of third-degree burn infection with bioluminescent Gram-negative bacteria was used to test the *in vivo* effectiveness of the therapeutic approach using the UVA excitation [105].

Our hypothesis was that the attachment of an additional deca(tertiary-ethylenylamino)malonate arm to C70, producing LC18, allowed the moiety to act as a potent electron donor and increased the generation yield of hydroxyl radicals under UVA illumination. This is consistent with the reported phenomena of photoinduced intramolecular electron transfer from the tertiary amine moiety to the fullerene cage in polar solvents, including water, at the short excitation wavelength.

Addition of a different inorganic salt, potassium iodide can also be used to strongly potentiate aPDI [106]. This is particularly important in the case of Gram-negative bacteria where many PS that cannot normally kill *E. coli,* can eradicate the cells (6 logs of killing) when KI is added. This has been shown for Photofrin [107] and Rose Bengal [108]. The mechanism was proposed to involve the oxidation of iodide to free iodine or reactive iodine radicals and can operate by both Type 1 or Type 2 photochemical mechanisms. In a study by Zhang et al [109] we showed that the microbial killing mediated by LC16 excited by either UVA or white light could be potentiated by additioion of KI (10 mM) in the case of Gram-negative *Acinetobacter baumannii*, MRSA and C. albicans. A mouse model infected with bioluminescent *A. baumannii* gave increased loss of bioluminescence when iodide (10 mM) was combined with LC16 and UVA/white light (Figure 10).

8 Fullerene-tetrapyrrole dyads

Photosynthesis which occurs in plants and in photosynthetic bacteria could be regarded as an elaborate, nano-scale, naturally occurring biological machine. The photosynthetic apparatus converts solar energy into chemical energy, that eventually forms the basic foodstuff for all

living organisms on the earth. The key process of photosynthesis is a cascade of photoinduced energy transfer and subsequent electron transfer reactions between donor and acceptor molecules in the antenna complexes and reaction centers. The final charge-separated state has a quantum efficiency of nearly 100%, as well as a lifetime of the order of seconds. Electrons are removed from suitable substrates, such as water, producing oxygen gas. The hydrogen freed by the splitting of water is used in the production of two intermediate compounds that serve as short-term stores of cellular energy (reduced nicotinamide adenine dinucleotide phosphate, NADPH, and adenosine triphosphate, ATP). NADPH and ATP can then be used to power the biosynthesis of sugars from carbon dioxide extracted from the air in the Calvin cycle for carbon fixation. The unique, nano-sized three-dimensional structure of the photosynthetic apparatus has inspired synthetic chemists who are searching for improved methods of solar energy conversion and light harvesting antennae [110].

One way of accomplishing this goal efficiently is to covalently join an efficient light-harvesting molecule (such as porphyrin) to a good electron acceptor molecule (such as a fullerene). A wide range of donor–bridge–acceptor hybrids have been synthesized to investigate which factors are important for light-driven energy and electron transfer. Porphyrin-fullerene dyads can be joined by flexible or rigid linkers, which can be linear or non-linear, and can contain aromatic rings, or double or triple carbon bonds. All of these factors have an important effect on the photophysical properties of the porphyrin-fullerene dyads [111, 112]. The process of energy and electron transfer was investigated by Kuclauskas et al [113]. In toluene, the porphyrin first excited singlet state had a lifetime about 20 ps and decayed by singlet–singlet energy transfer to the fullerene. The fullerene first excited singlet state underwent intersystem crossing to the triplet, which exists in equilibrium with the porphyrin triplet state. In benzonitrile, photoinduced electron transfer from the porphyrin first excited singlet state to the fullerene competed with energy transfer. The fullerene excited singlet state was also quenched by electron transfer from the porphyrin. Overall, the charge-separated state was produced with a quantum yield approaching unity. Onal and coworkers conducted a structure-function analysis of the singlet oxygen quantum yield in porphyrin-fullerene dyads dissolved in toluene [114]. The molecular orbital levels and energy gaps of the dyads were determined by electrochemistry and theoretical calculations. The presence of an electron-donating hexyloxy chain at the para position of the meso-phenyl groups on the porphyrin, and the presence of a phenylacetylene spacer encouraged generation of singlet oxygen.

Milanesio et al [73] used tetrapyrrole-fullerene conjugates and evaluated PDT effect with a porphyrin-C_{60} dyad (P-C_{60}) and its metal complex with Zn(II) (ZnP-C_{60}) and compared with 5-(4-acetamidophenyl)-10,15,20-tris(4-methoxyphenyl)porphyrin (P) on Hep-2 human larynx carcinoma cell line. The phototoxicity was dependent on light exposure level with visible light. 80% phototoxicity was observed for P-C_{60} after 15 min of light irradiation which was higher as compared to ZnP-C_{60}. In the presence of an argon atmosphere a high photoactivity was observed with both the dyads. In another paper [74] the cell death was confirmed to occur by apoptotic mode.

Fullerene-tetrapyrrole dyads have also been tested to overcome the requirement to utilize UV or short-wavelength visible light to activate fullerenes. In one study where two new fullerene-bis-pyropheophorbide-a derivatives were prepared: a mono-(FP1) and a hexaadduct (FHP1.) The C_{60} hexaadduct FHP1 had a significant phototoxic activity (58% cell death, after a dose of 400 mJ/cm^2 of 688 nm light) but the monoadduct FP1 had a very low phototoxicity and only at higher light doses. Nevertheless, the activity of both adducts was less than that of pure pyropheophorbide-a, possibly due to the lower cellular uptake of the adducts [115].

9 Advanced fullerene-based nanostructures and theranostics

In common with a large number of other investigations in the nanomedicine sphere, the concepts of multifunctionality and theranostics has spread to include fullerenes as well. Over recent years, a great variety of nanoparticles have been employed as drug delivery vehicles and imaging vehicles in anticancer therapeutics. Suitable nanoparticles can show unique pharmacokinetics (including minimal renal filtration, which in turn extends circulation time in the blood, depending on the surface functionalization [116]), they have high surface area to volume ratio (that enables them to be modified with various functional groups), and they possess the possibility to attach tailored functionalities. These properties taken together have made nanoparticles enormously attractive for medical applications. Nanoparticle-constructs can possess the simultaneous abilities to home to a target, allow real time imaging, deliver therapeutics, and monitor the results of the therapy, which is the definition of “theranostics”. The ability to finely tune the timing and dosage of therapeutic agents, and the timing of an external activation agent (light, heat or ultrasound) and thus produce truly individualized medicine, as opposed to adopting a ‘one-size-fits-all’ approach as in the past.

To produce theranostic nanoparticles, various therapeutic strategies, such as nucleic acid therapeutics for gene therapy, chemotherapeutic drugs, hyperthermia (photothermal ablation), photodynamic therapy, radiation therapy or therapeutic ultrasound have been combined with one or more imaging functionalities. Drug or gene delivery vehicles can be decorated with different imaging probes, such as MRI contrast agents (T1 and T2 agents), fluorescent markers (organic dyes and inorganic quantum dots), photoacoustic reporters, Raman probes, or nuclear imaging agents (PET/SPECT/CT) in order to facilitate imaging, and in doing so, gain information about the trafficking pathways, kinetics of delivery, and therapeutic efficacy.

The present review will briefly cover some examples of multifunctional and theranostic nanoparticles where fullerenes have played a major role. Guan et al [117] reported a novel “phototheranostic” platform based on tri-malonate derivative of fullerene C70 that self-assembled into nanovesicles (FCNVs) that could be loaded with the photosensitizer (chlorin e6, Ce6). The amphiphilic TFC70-oligo ethylene glycol-Ce6 FCNVs possessed the following advantages: (i) high loading efficiency of Ce6 (up to ~57 wt%); (ii) efficient absorption in the red light spectrum; (iii) enhanced cellular uptake; (iv) high PDT efficiency of Ce6 in vitro and in vivo; (v) ability to allow in vivo fluorescence imaging; (vi) good biocompatibility and total elimination from the body.

Shi and co-workers [118] reported the preparation of fullerene (C60)-based tumor-targeting nanoparticles with a controllable “off-on state”. Doxorubicin (DOX) was covalently conjugated to fullerene (C60) nanoaggregates via a reactive oxygen species (ROS)-sensitive thioketal linker (C60-DOX NPs), and then a hydrophilic coating (distearoyl-sn-glycero-3-phosphoethanolamine-PEG-CNGRCK2HK3HK11, DSPE-PEG-NGR) was attached to the outer surface of C60-DOX providing stability in physiological solutions and an active tumor-targeting capacity. C60-DOX-NGR NPs were able to entrap DOX efficiently even in an acidic environment (pH 5.5) when they were in the “off” state. In contrast, when the NPs were in the “on” state when they were irradiated by a 532nm laser (at low power density) with high spatial/temporal resolution, a large amount of ROS was generated, leading to the breaking of the ROS-sensitive linkers, and the burst release of DOX. The “off” or “on” state of the C60-DOX-NGR NPs could be precisely remote-controlled by the laser irradiation. In vivo these nanoparticles showed a high antitumor efficacy and a low toxicity to normal tissues.

Du and colleagues [119] described a nanocomposite composed of N-succinyl-N′-4-(2-nitrobenzyloxy)-succinyl-chitosan micelles (SNSC) loaded with fullerene (C60), iron oxide (Fe_3O_4) nanoparticles and upconversion nanophosphors (UCNPs). In addition, the hydrophobic anticancer drug docetaxel (DTX) was also loaded into the nanocomposites. The experiments conducted in vitro and in vivo demonstrated that C60/Fe_3O_4-UCNPs@DTX@SNSC could act synergistically to kill tumor cells by releasing chemotherapy drugs at a specific target site, in addition to generating ROS when excited by a 980 nm laser. Non-invasive dual-mode imaging employed both magnetic resonance imaging and upconversion fluorescence imaging.

Wang et al [120] studied multifunctional nanoparticles to target cancer stem cells (CSCs). CSCs are resistant to chemotherapy and are highly tumorigenic, which contributes to tumor growth and relapse and spread post-treatment. They prepared a C60 fullerene-silica nanoparticle system decorated with hyaluronan (HA) on the surface to target the CD44 variant (hyaluronan receptor) overexpressed on breast CSCs. Doxorubicin hydrochloride (DOX) and indocyanine green (ICG) were encapsulated in the nanoparticles to provide combined chemo (DOX), photodynamic (C60), and photothermal (ICG) therapy using near infrared laser (810 nm) irradiation. Nanoparticles with a higher drug loading content (e.g., 48.5 versus 4.6%) had significantly higher antitumor efficacy, given the same total drug dose.

Li and his team [121] prepared a graphene oxide-fullerene C60 (GO-C60) hybrid that could carry out photodynamic therapy (PDT) and photothermal therapy (PTT) at the same time. Using a stepwise conjugation method, GO-C_{60} containing hydrophilic methoxypolyethylene glycol (mPEG) and mono-substituted C_{60} was synthesized. The introduction of C_{60} to GO did not decrease the photothermal properties of GO, while the conjugation of GO to C_{60} increased the ability of C_{60} to generate $^1O_2$ under NIR laser. Due to the synergistic effect between GO and C_{60}, the GO-C_{60} hybrid exhibited superior killing of cancer cells compared to either compound individually. Other systems have also shown that PDT and hyperthermia are synergistic [122, 123]. Finally, Shi et al [124] combined fullerene (C60) and gold nanoparticles (AuNPs) that were functionalized by PEG5000 using a pH-cleavable

hydrazone bond, producing C60@Au-PEG. The goal was to maintain on the surface during blood circulation but allow PEG to dissociate after accumulation in tumor tissue. Doxorubicin (DOX) was loaded onto C60@Au-PEG with high efficiency. The release profile of DOX from C60@Au-PEG/DOX showed strong dependence on radio frequency (RF) irradiation. C60@Au-PEG/DOX showed a higher antitumor efficacy owing to 8.6-fold higher DOX uptake of tumor compared to free DOX. C60@Au-PEG/DOX not only allowed RF-thermal tumor ablation and was a powerful photosensitizer (PS) for visible-light activated PDT, but also acted as as an X-ray contrast agent for tumor diagnosis. Triple combination therapy (chemo-RF thermal-PDT), RF-controlled drug release, tumor targeting, acid mediated PEG release and X-ray contrast agent made a truly multi-functional theranostic agent.

Upconversion is a physical phenomenon in which certain rare-earth metal cations can combine to change long wavelength NIR light into shorter wavelength visible light. Unlike two-photon absorption which requires very short-pulsed lasers, upconversion works with CW light. The mechanism involves a ytterbium cation absorbing several successive 980 nm photons and transferring the energy to a second cation (for instance erbium) which can reemit the energy as visible light. In order to maintain these rare earth ions adjacent to each other they are fixed into nanoparticles made from sodium yttrium fluoride (UCNPs) that also incorporate the PS needed to produce ROS from the upconverted light. The net result is much deeper tissue penetration of the light [125]. Liu et al used separately dual-doped (Yb^{3+}:Er^{3+} and Yb^{3+}:Tm^{3+}) UCNPs to take advantage of the broad-spectrum light harvesting ability of fullerenes [126]. The 70 nm NPs-PEG-$NaYF_4$:Yb^{3+},Er^{3+}/ $NaYF_4$:Yb^{3+},Tm^{3+} targeted with folic acid attached to the outside and covalently conjugated to monomalonic C60 fullerene (C60MA) were employed to kill HeLa cells after 980 nm excitation.

10 Pros and cons of fullerenes for PDT

There are an astonishing variety of chemical structures that could theoretically be employed as PDT agents of one sort or another. The goal of this review is to guide investigators which properties of fullerenes are particularly suitable for PDT applications, and what are the disadvantages associated with fullerene-mediated PDT that may be pitfalls for the unwary.

Pros

1. The highly versatile chemical structure of fullerenes allows many different functional groups to be attached by facile reactions such as the Bingel and Prato reactions. Moreover, a large number of the double bonds present in the molecule would need to be altered to single bonds by functionalization in order to seriously reduce the optical absorption characteristics and photophysical properties.
2. Fullerenes can be attached to light harvesting antennae and electron transfer dyads to change the wavelengths of absorption towards the red end of the spectrum. These attached antennae can encourage charge separation mechanisms and electron transfer mechanisms.

3. Fullerenes are able to carry out Type 1, Type 2 and electron transfer photochemical reactions the balance of which can be tailored by appropriate modification, making them more versatile than most other PS chemical structures that are used in PDT applications. In biological environments, singlet oxygen (Type II) plays only a minor role in many killing functions mediated by photoactivated fullerenes.

4. Due to the electron transfer mechanisms, there is the possibility of oxygen independent photoinactivation. This may be important for instance in the use of aPDI to kill anaerobic bacteria that are responsible for a variety of human infections in anatomical areas that have intrinsically

5. When used as antimicrobial PS, fullerenes can be strongly potentiated by the addition of the non-toxic salt, KI. Potentiation by other inorganic salts (nitrite, thiocyanate, selenocyanate) is also possible.

6. The spherical shape typical of fullerene molecules can undergo self-assembly into interesting supramolecular nanostructures such as “fullerosomes”.

7. Fullerenes can act as constituents of multifunctional theranostic nanostructures that have been widely studies in the modern explosion of nanotechnology.

8. Fullerenes are highly resistant to photobleaching. Many traditional PS structures are totally destroyed, or completely lose their photoactivity by a relatively low total energy dose (< 10 J/cm2) while fullerenes can retain PDT activity after very high fluences (> 1000 J/cm2).

Cons

1. Pristine fullerenes are highly hydrophobic with a propensity to aggregate in aqueous environments. Even when they are functionalized with water-soluble polar groups, this drawback may not entirely overcome.

2. The absorption spectrum of fullerenes is heavily biased towards the UV and blue part of the spectrum so light penetration into tissue will always be problematic [127].

   To overcome this obstacle high-tech optical approaches have been investigated such as two-photon excitation. This involves the use of a short-pulsed (femtosecond) laser so that simultaneous absorption of two NIR photons (e.g. 808 nm) will be equivalent to absorption of a single 404 nm photon, but at much greater depth [128]. Another technique is rare-earth mediated upconversion where a nanoparticle containing lanthanide ions) e.g. ytterbium and erbium) allows the absorption of several long wavelength photons from a CW laser (for instance 980 nm), and the upconverted emission of shorter blue or green photons [125].

3. C60 itself has a relatively high molecular weight (720). When substantial additional moieties are conjugated to the cage the MWt can rise significantly. For instance, the MWts of LC15, LC16, LC18 and LC 20 are 3755, 4211, 4334 and 4890 respectively. Uptake of molecules this large into cells is beset with

difficulties, and in fact these molecules have lower activity than expected against different bacteria probably because their large molecular size restricts the degree to which they can penetrate into bacterial cell walls. A similar result was seen with a chlorophyll derivative that was also equipped with these deca-cationic chains [129].

4. As mentioned previously there the paradoxical possibility that fullerenes can act as strong oxidizing agents when excited with light in the presence of oxygen, but may also act as anti-oxidants in the dark. At the present time, it is unclear how much this interesting contradiction affects the ability of fullerenes to act as effective PDT agents.

5. Fullerenes are generally not fluorescent [130] although some papers do claim that fluorescence microscopy can be used to visualize the sub-cellular localization of various fullerene derivatives [131].

Acknowledgments

MRH was supported by US NIH grants R01AI050875 and R21AI121700

References

1. Osawa E, Kroto HW, Fowler PW, et al. The Evolution of the Football Structure for the C60 Molecule: A Retrospective [and Discussion]. Philosophical Transactions: Physical Sci. 1993; 343:1–8.
2. Baggott J. Perfect Symmetry - The Accidental Discovery of Buckminsterfullerene. Oxford, UK: Oxford University Press; 1994.
3. Thrower PA. Editorial. Carbon. 1999; 37:1677–8.
4. Bochvar DA, Galpern EG. On hypothetical systems: carbon dodecahedron, S-icosahedron and carbon-S-icosahedron. Dokl Acad Nauk SSSR. 1973; 209:610.
5. The Nobel Prize in Chemistry. 1996. https://www.nobelprize.org/nobel_prizes/chemistry/laureates/1996/
6. Wang S, Yang S, Kemnitz E, et al. New Giant Fullerenes Identified as Chloro Derivatives: Isolated-Pentagon-Rule C108(1771)Cl12 and C106(1155)Cl24 as well as Nonclassical C104Cl24. Inorg Chem. 2016; 55:5741–3. [PubMed: 27276659]
7. Bosi S, Da Ros T, Spalluto G, et al. Fullerene derivatives: an attractive tool for biological applications. EurJMedChem. 2003; 38:913–23.
8. Jensen AW, Wilson SR, Schuster DI. Biological applications of fullerenes. BioorgMedChem. 1996; 4:767–79.
9. Tagmatarchis N, Shinohara H. Fullerenes in medicinal chemistry and their biological applications. Mini RevMedChem. 2001; 1:339–48.
10. Von Tappenier H. Uber die Wirkung fluoreszierender Stoffe auf Infusorien nach Versuchen von O. Raab Muench Med Wochenschr. 1900; 47:5.
11. Von Tappeiner H, Jodlbauer A. Uber Wirkung der photodynamischen (fluorieszierenden) Stoffe auf Protozoan und Enzyme. Dtsch Arch Klin Med. 1904; 80:427–87.
12. Hausman W. Die sensibilisierende wirkung des hematoporphyrins. Biochem Z. 1911; 30:276.
13. Weishaupt KR, Gomer CJ, Dougherty TJ. Identification of singlet oxygen as the cytotoxic agent in photoinactivation of a murine tumor. Cancer Res. 1976; 36:2326–9. [PubMed: 1277137]
14. Ochsner M. Photophysical and photobiological processes in the photodynamic therapy of tumours. J Photochem Photobiol B. 1997; 39:1–18. [PubMed: 9210318]
15. da Silva Baptista M, Cadet J, Di Mascio P, et al. Type I and II Photosensitized Oxidation Reactions: Guidelines and Mechanistic Pathways. Photochem Photobiol. 2017

16. Garcia-Diaz M, Huang YY, Hamblin MR. Use of fluorescent probes for ROS to tease apart Type I and Type II photochemical pathways in photodynamic therapy. Methods. 2016; 109:158–66. [PubMed: 27374076]
17. Hamblin MR. Antimicrobial photodynamic inactivation: a bright new technique to kill resistant microbes. Curr Opin Microbiol. 2016; 33:67–73. [PubMed: 27421070]
18. Mroz P, Tegos GP, Gali H, et al. Photodynamic therapy with fullerenes. Photochem Photobiol Sci. 2007; 6:1139–49. [PubMed: 17973044]
19. Foote CS. Photophysical and photochemical properties of fullerenes. Top Curr Chem. 1994; 169:347–63.
20. Greer A. Christopher Foote's discovery of the role of singlet oxygen [1O2 (1Delta g)] in photosensitized oxidation reactions. Acc Chem Res. 2006; 39:797–804. [PubMed: 17115719]
21. Schmidt R. Photosensitized generation of singlet oxygen. Photochem Photobiol. 2006; 82:1161–77. [PubMed: 16683906]
22. Arbogast JW, Darmanyan AP, Foote CS, et al. Photophysical properties of C60. J Phys Chem A. 1991; 95:11–2.
23. Yamakoshi Y, Umezawa N, Ryu A, et al. Active oxygen species generated from photoexcited fullerene (C60) as potential medicines: O2-* versus 1O2. J Am Chem Soc. 2003; 125:12803–9. [PubMed: 14558828]
24. Foote CS. Definition of Type-I and Type-II photosensitized oxidation. Photochem Photobiol. 1991; 54:659. [PubMed: 1798741]
25. Koeppe R, Sariciftci NS. Photoinduced charge and energy transfer involving fullerene derivatives. Photochem Photobiol Sci. 2006; 5:1122–31. [PubMed: 17136277]
26. Guldi DM, Prato M. Excited-state properties of C(60) fullerene derivatives. Acc Chem Res. 2000; 33:695–703. [PubMed: 11041834]
27. Arbogast JW, Foote CS, Kao M. Electron-transfer to triplet C-60. J Am Chem Soc. 1992; 114:2277–9.
28. Miyata N, Yamakoshi Y, Nakanishi I. Reactive species responsible for biological actions of photoexcited fullerenes. Yakugaku Zasshi. 2000; 120:1007–16. [PubMed: 11082711]
29. Gharbi N, Pressac M, Hadchouel M, et al. [60]fullerene is a powerful antioxidant in vivo with no acute or subacute toxicity. Nano Lett. 2005; 5:2578–85. [PubMed: 16351219]
30. Andrievsky GV, Bruskov VI, Tykhomyrov AA, et al. Peculiarities of the antioxidant and radioprotective effects of hydrated C60 fullerene nanostuctures in vitro and in vivo. Free radical biology & medicine. 2009; 47:786–93. [PubMed: 19539750]
31. Avdeev MV, Khokhryakov AA, Tropin TV, et al. Structural features of molecular-colloidal solutions of C60 fullerenes in water by small-angle neutron scattering. Langmuir: the ACS journal of surfaces and colloids. 2004; 20:4363–8. [PubMed: 15969139]
32. Bingel C. Cyclopropanierung von Fullerenen. Chemische Berichte. 1993; 126:1957.
33. Gothelf AS, Gothelf KV, Hazell RG, et al. Catalytic asymmetric 1,3-dipolar cycloaddition reactions of azomethine ylides-a simple approach to optically active highly functionalized proline derivatives. Angew Chem Int Ed Engl. 2002; 41:4236–8. [PubMed: 12434349]
34. Maggini M, Scorrano G, Prato M. The Addition of Azomethine Ylides to C60: Synthesis, Characterization and Functionalization of Fullerene-Pyrrolidines. J Am Chem Soc. 1993; 115:9798–9.
35. Yu C, Canteenwala T, El-Khouly ME, et al. Efficiency of singlet oxygen production from self-assembled nanospheres of molecular micelle-like photosensitizers FC4S. J Mater Chem. 2005; 15:857–1864.
36. Nakamura E, Isobe H. Functionalized fullerenes in water. The first 10 years of their chemistry, biology, and nanoscience. Accounts of chemical research. 2003; 36:807–15. [PubMed: 14622027]
37. Yurovskaya M, Trushkov I. Cycloaddition to buckminsterfullerene C60: advancements and future prospects. Russ Chem Bull. 2002; 51:367–443.
38. Maggini M, Scorrano G, Prato M. Addition of azomethine ylides to C60: synthesis, characterization, and functionalization of fullerene pyrrolidines. J Am Chem Soc. 1993; 115:9798–9.

39. Wang M, Huang L, Sharma SK, et al. Synthesis and photodynamic effect of new highly photostable decacationically armed [60]- and [70]fullerene decaiodide monoadducts to target pathogenic bacteria and cancer cells. J Med Chem. 2012; 55:4274–85. [PubMed: 22512669]
40. Sperandio FF, Sharma SK, Wang M, et al. Photoinduced electron-transfer mechanisms for radical-enhanced photodynamic therapy mediated by water-soluble decacationic C(7)(0) and C(8)(4)O(2) Fullerene Derivatives. Nanomedicine NBM. 2013; 9:570–9.
41. Brettreich M, Burghardt S, Bottcher C, et al. Globular Amphiphiles: Membrane-Forming Hexaadducts of C(60) This work was been supported by the Deutsche Forschungsgemeinschaft and by the Fonds der Chemischen Industrie. We thank Dr. K. Fischer and Prof. Dr. K. Schmidt from the Institute of Physical Chemistry at the University of Mainz for performing the light scattering measurements. Angew Chem Int Ed Engl. 2000; 39:1845–8. [PubMed: 10934382]
42. Lu Z, Dai T, Huang L, et al. Photodynamic therapy with a cationic functionalized fullerene rescues mice from fatal wound infections. Nanomedicine: nanotechnology, biology, and medicine. 2010; 5:1525–33.
43. Mizuno K, Zhiyentayev T, Huang L, et al. Antimicrobial Photodynamic Therapy with Functionalized Fullerenes: Quantitative Structure-activity Relationships. Journal of nanomedicine & nanotechnology. 2011; 2:1–9.
44. Wang M, Maragani S, Huang L, et al. Synthesis of decacationic [60]fullerene decaiodides giving photoinduced production of superoxide radicals and effective PDT-mediation on antimicrobial photoinactivation. Eur J Med Chem. 2013; 63:170–84. [PubMed: 23474903]
45. Thota S, Wang M, Jeon S, et al. Synthesis and characterization of positively charged pentacationic [60]fullerene monoadducts for antimicrobial photodynamic inactivation. Molecules. 2012; 17:5225–43. [PubMed: 22565476]
46. Chiang LY, Padmawar PA, Rogers-Haley JE, et al. Synthesis and characterization of highly photoresponsive fullerenyl dyads with a close chromophore antenna-C(60) contact and effective photodynamic potential. J Mater Chem. 2010; 20:5280–93. [PubMed: 20890406]
47. El-Khouly ME, Padmawar P, Araki Y, et al. Photoinduced processes in a tricomponent molecule consisting of diphenylaminofluorene-dicyanoethylene-methano[60]fullerene. J Phys Chem A. 2006; 110:884–91. [PubMed: 16419985]
48. Kato S, Aoshima H, Saitoh Y, et al. Fullerene-C60/liposome complex: Defensive effects against UVA-induced damages in skin structure, nucleus and collagen type I/IV fibrils, and the permeability into human skin tissue. J Photochem Photobiol B. 2010; 98:99–105. [PubMed: 20036139]
49. Doi Y, Ikeda A, Akiyama M, et al. Intracellular uptake and photodynamic activity of water-soluble [60]- and [70]fullerenes incorporated in liposomes. Chemistry. 2008; 14:8892–7. [PubMed: 18698574]
50. Yan A, Von Dem Bussche A, Kane AB, et al. Tocopheryl Polyethylene Glycol Succinate as a Safe, Antioxidant Surfactant for Processing Carbon Nanotubes and Fullerenes. Carbon N Y. 2007; 45:2463–70. [PubMed: 19081834]
51. Akiyama M, Ikeda A, Shintani T, et al. Solubilisation of [60]fullerenes using block copolymers and evaluation of their photodynamic activities. Org Biomol Chem. 2008; 6:1015–9. [PubMed: 18327326]
52. Kojima C, Toi Y, Harada A, et al. Aqueous solubilization of fullerenes using poly(amidoamine) dendrimers bearing cyclodextrin and poly(ethylene glycol). Bioconjugate chemistry. 2008; 19:2280–4. [PubMed: 18844391]
53. Pan B, Cui D, Xu P, et al. Synthesis and characterization of polyamidoamine dendrimer-coated multi-walled carbon nanotubes and their application in gene delivery systems. Nanotechnology. 2009; 20:125101. [PubMed: 19420458]
54. Hooper JB, Bedrov D, Smith GD. Supramolecular self-organization in PEO-modified C60 fullerene/water solutions: influence of polymer molecular weight and nanoparticle concentration. Langmuir: the ACS journal of surfaces and colloids. 2008; 24:4550–7. [PubMed: 18402490]
55. Nitta N, Seko A, Sonoda A, et al. Is the use of fullerene in photodynamic therapy effective for atherosclerosis? Cardiovascular and interventional radiology. 2008; 31:359–66. [PubMed: 18040738]

56. Liu J, Ohta S, Sonoda A, et al. Preparation of PEG-conjugated fullerene containing Gd3+ ions for photodynamic therapy. Journal of controlled release: official journal of the Controlled Release Society. 2007; 117:104–10. [PubMed: 17156882]
57. Tabata Y, Murakami Y, Ikada Y. Photodynamic effect of polyethylene glycol-modified fullerene on tumor. Japanese journal of cancer research: Gann. 1997; 88:1108–16. [PubMed: 9439687]
58. Bali V, Ali M, Ali J. Novel nanoemulsion for minimizing variations in bioavailability of ezetimibe. Journal of drug targeting. 2010; 18:506–19. [PubMed: 20067438]
59. Amani A, York P, Chrystyn H, et al. Factors affecting the stability of nanoemulsions--use of artificial neural networks. Pharmaceutical research. 2010; 27:37–45. [PubMed: 19908130]
60. Bansal T, Mustafa G, Khan ZI, et al. Solid self-nanoemulsifying delivery systems as a platform technology for formulation of poorly soluble drugs. Critical reviews in therapeutic drug carrier systems. 2008; 25:63–116. [PubMed: 18540836]
61. Shakeel F, Faisal MS. Nanoemulsion: a promising tool for solubility and dissolution enhancement of celecoxib. Pharmaceutical development and technology. 2010; 15:53–6. [PubMed: 19552546]
62. Filippone S, Heimann F, Rassat A. A highly water-soluble 2:1 beta-cyclodextrin-fullerene conjugate. Chemical communications. 2002:1508–9. [PubMed: 12189867]
63. Zhao B, He YY, Bilski PJ, et al. Pristine (C60) and hydroxylated [C60(OH)24] fullerene phototoxicity towards HaCaT keratinocytes: type I vs type II mechanisms. Chemical research in toxicology. 2008; 21:1056–63. [PubMed: 18422350]
64. Agostinis P, Berg K, Cengel KA, et al. Photodynamic therapy of cancer: An update. CA Cancer J Clin. 2011; 61:250–81. [PubMed: 21617154]
65. Dougherty TJ. Photodynamic therapy (PDT) of malignant tumors. Crit Rev Oncol Hematol. 1984; 2:83–116. [PubMed: 6397270]
66. Dougherty TJ. A brief history of clinical photodynamic therapy development at Roswell Park Cancer Institute. J Clin Laser Med Surg. 1996; 14:219–21. [PubMed: 9612186]
67. Foley S, Crowley C, Smaihi M, et al. Cellular localisation of a water-soluble fullerene derivative. Biochemical and biophysical research communications. 2002; 294:116–9. [PubMed: 12054749]
68. Burlaka AP, Sidorik YP, Prylutska SV, et al. Catalytic system of the reactive oxygen species on the C60 fullerene basis. Experimental oncology. 2004; 26:326–7. [PubMed: 15627068]
69. Rancan F, Rosan S, Boehm F, et al. Cytotoxicity and photocytotoxicity of a dendritic C(60) mono-adduct and a malonic acid C(60) tris-adduct on Jurkat cells. Journal of photochemistry and photobiology B, Biology. 2002; 67:157–62.
70. Rancan F, Helmreich M, Molich A, et al. Fullerene-pyropheophorbide a complexes as sensitizer for photodynamic therapy: uptake and photo-induced cytotoxicity on Jurkat cells. J Photochem Photobiol B. 2005; 80:1–7. [PubMed: 15963432]
71. Granville DJ, Carthy CM, Jiang H, et al. Rapid cytochrome c release, activation of caspases 3, 6, 7 and 8 followed by Bap31 cleavage in HeLa cells treated with photodynamic therapy. FEBS Lett. 1998; 437:5–10. [PubMed: 9804161]
72. Gupta S, Ahmad N, Mukhtar H. Involvement of nitric oxide during phthalocyanine (Pc4) photodynamic therapy-mediated apoptosis. Cancer Res. 1998; 58:1785–8. [PubMed: 9581812]
73. Milanesio ME, Alvarez MG, Rivarola V, et al. Porphyrin-fullerene C60 dyads with high ability to form photoinduced charge-separated state as novel sensitizers for photodynamic therapy. Photochem Photobiol. 2005; 81:891–7. [PubMed: 15757366]
74. Alvarez MG, Prucca C, Milanesio ME, et al. Photodynamic activity of a new sensitizer derived from porphyrin-C60 dyad and its biological consequences in a human carcinoma cell line. Int J Biochem Cell Biol. 2006; 38:2092–101. [PubMed: 16899389]
75. Chen HH, Yu C, Ueng TH, et al. Acute and subacute toxicity study of water-soluble polyalkylsulfonated C60 in rats. Toxicologic pathology. 1998; 26:143–51. [PubMed: 9502397]
76. Yu C, Canteenwala T, Chen H, et al. Hexa (sulfobutyl) fullerene-induced photodynamic effect on tumors in vivo and toxicity study in rats. Proc Electrochem Soc. 1999; 99:234–49.
77. Mroz P, Xia Y, Asanuma D, et al. Intraperitoneal photodynamic therapy mediated by a fullerene in a mouse model of abdominal dissemination of colon adenocarcinoma. Nanomedicine: nanotechnology, biology, and medicine. 2011; 7:965–74.

78. Otake E, Sakuma S, Torii K, et al. Effect and mechanism of a new photodynamic therapy with glycoconjugated fullerene. Photochemistry and photobiology. 2010; 86:1356–63. [PubMed: 20796243]
79. O'Neill J. The Review on Antimicrobial Resistance Chaired by Jim O'Neill. 2015. Tackling a global health crisis:initial steps.
80. Maisch T. A new strategy to destroy antibiotic resistant microorganisms: antimicrobial photodynamic treatment. Mini Rev Med Chem. 2009; 9:974–83. [PubMed: 19601890]
81. Talan DA. MRSA: deadly super bug or just another staph? Ann Emerg Med. 2008; 51:299–302. [PubMed: 18222565]
82. Livermore DM. Has the era of untreatable infections arrived? J Antimicrob Chemother. 2009; 64(Suppl 1):i29–36. [PubMed: 19675016]
83. Hughes D, Karlen A. Discovery and preclinical development of new antibiotics. Ups J Med Sci. 2014; 119:162–9. [PubMed: 24646082]
84. Donadio S, Maffioli S, Monciardini P, et al. Antibiotic discovery in the twenty-first century: current trends and future perspectives. J Antibiot (Tokyo). 2010; 63:423–30. [PubMed: 20551985]
85. Hamblin MR, Hasan T. Photodynamic therapy: a new antimicrobial approach to infectious disease? PhotochemPhotobiolSci. 2004; 3:436–50.
86. Hancock RE, Bell A. Antibiotic uptake into gram-negative bacteria. Eur J Clin Microbiol Infect Dis. 1988; 7:713–20. [PubMed: 2850910]
87. Martin JP, Logsdon N. The role of oxygen radicals in dye-mediated photodynamic effects in Escherichia coli B. J Biol Chem. 1987; 262:7213–9. [PubMed: 3034885]
88. Culotta L, Koshland DE Jr. Buckyballs: wide open playing field for chemists. Science. 1991; 254:1706–9. [PubMed: 17829222]
89. Duncan LK, Jinschek JR, Vikesland PJ. C60 colloid formation in aqueous systems: effects of preparation method on size, structure, and surface charge. Environ Sci Technol. 2008; 42:173–8. [PubMed: 18350893]
90. Tegos GP, Demidova TN, Arcila-Lopez D, et al. Cationic fullerenes are effective and selective antimicrobial photosensitizers. ChemBiol. 2005; 12:1127–35.
91. Mashino T, Usui N, Okuda K, et al. Respiratory chain inhibition by fullerene derivatives: hydrogen peroxide production caused by fullerene derivatives and a respiratory chain system. Bioorganic & medicinal chemistry. 2003; 11:1433–8. [PubMed: 12628669]
92. Mashino T, Okuda K, Hirota T, et al. Inhibition of E. coli growth by fullerene derivatives and inhibition mechanism. Bioorganic & medicinal chemistry letters. 1999; 9:2959–62. [PubMed: 10571155]
93. Spesia MB, Milanesio ME, Durantini EN. Synthesis, properties and photodynamic inactivation of Escherichia coli by novel cationic fullerene C60 derivatives. Eur J Med Chem. 2008; 43:853–61. [PubMed: 17706838]
94. Dai T, Huang YY, Sharma SK, et al. Topical antimicrobials for burn wound infections. Recent patents on anti-infective drug discovery. 2010; 5:124–51. [PubMed: 20429870]
95. Dahl TA, Midden WR, Hartman PE. Comparison of killing of gram-negative and gram-positive bacteria by pure singlet oxygen. Journal of bacteriology. 1989; 171:2188–94. [PubMed: 2703469]
96. Valduga G, Bertoloni G, Reddi E, et al. Effect of extracellularly generated singlet oxygen on gram-positive and gram-negative bacteria. J Photochem Photobiol B. 1993; 21:81–6. [PubMed: 8289115]
97. Huang L, Xuan Y, Koide Y, et al. Type I and Type II mechanisms of antimicrobial photodynamic therapy: An in vitro study on gram-negative and gram-positive bacteria. Lasers Surg Med. 2012; 44:490–9. [PubMed: 22760848]
98. Kashef N, Huang YY, Hamblin MR. Advances in antimicrobial photodynamic inactivation at the nanoscale. Nanophotonics. 2017; 6:853–79. [PubMed: 29226063]
99. Huang L, St Denis TG, Xuan Y, et al. Paradoxical potentiation of methylene blue-mediated antimicrobial photodynamic inactivation by sodium azide: role of ambient oxygen and azide radicals. Free radical biology & medicine. 2012; 53:2062–71. [PubMed: 23044264]

100. Kasimova KR, Sadasivam M, Landi G, et al. Potentiation of photoinactivation of Gram-positive and Gram-negative bacteria mediated by six phenothiazinium dyes by addition of azide ion. Photochem Photobiol Sci. 2014; 13:1541–8. [PubMed: 25177833]
101. Yin R, Wang M, Huang YY, et al. Antimicrobial photodynamic inactivation with decacationic functionalized fullerenes: oxygen independent photokilling in presence of azide and new mechanistic insights. Free radical biology & medicine. 2015; 79:14–27. [PubMed: 25451642]
102. Tegos GP, Demidova TN, Arcila-Lopez D, et al. Cationic fullerenes are effective and selective antimicrobial photosensitizers. Chem Biol. 2005; 12:1127–35. [PubMed: 16242655]
103. Ollstein RN, McDonald C. Topical and systemic antimicrobial agents in burns. Ann Plast Surg. 1980; 5:386–92. [PubMed: 6779699]
104. Saffle JR. Closure of the excised burn wound: temporary skin substitutes. Clinics in plastic surgery. 2009; 36:627–41. [PubMed: 19793557]
105. Huang L, Wang M, Dai T, et al. Antimicrobial photodynamic therapy with decacationic monoadducts and bisadducts of [70]fullerene: in vitro and in vivo studies. Nanomedicine: nanotechnology, biology, and medicine. 2013
106. Hamblin MR. Potentiation of antimicrobial photodynamic inactivation by inorganic salts. Expert Rev Anti Infect Ther. 2017:1–11.
107. Huang L, Szewczyk G, Sarna T, et al. Potassium Iodide Potentiates Broad-Spectrum Antimicrobial Photodynamic Inactivation Using Photofrin. ACS Infect Dis. 2017; 3:320–8. [PubMed: 28207234]
108. Wen X, Zhang X, Szewczyk G, et al. Potassium Iodide Potentiates Antimicrobial Photodynamic Inactivation Mediated by Rose Bengal in In Vitro and In Vivo Studies. Antimicrob Agents Chemother. 2017:61.
109. Zhang Y, Dai T, Wang M, et al. Potentiation of antimicrobial photodynamic inactivation mediated by a cationic fullerene by added iodide: in vitro and in vivo studies. Nanomedicine: nanotechnology, biology, and medicine. 2015; 10:603–14.
110. Gust D, Moore TA, Moore AL. Mimicking photosynthetic solar energy transduction. Acc Chem Res. 2001; 34:40–8. [PubMed: 11170355]
111. Koji Y, Hiroshi I, Yoshinobu N, et al. Acceleration of Photoinduced Charge Separation in Porphyrin-C60 Dyad with an Acetylene Spacer. Chemistry Letters. 28:895–6.
112. Schuster DI, MacMahon S, Guldi DM, et al. Synthesis and photophysics of porphyrin–fullerene donor–acceptor dyads with conformationally flexible linkers. Tetrahedron. 2006; 62:1928–36.
113. Kuciauskas D, Lin S, Seely GR, et al. Energy and Photoinduced Electron Transfer in Porphyrin–Fullerene Dyads. J Phys Chem. 1996; 100:15926–32.
114. Onal E, Topal SZ, Fidan I, et al. Structure-Photoproperties Relationship Investigation of the Singlet Oxygen Formation in Porphyrin-Fullerene Dyads. J Fluoresc. 2017; 27:1855–69. [PubMed: 28667370]
115. Li R, Bounds DJ, Granville D, et al. Rapid induction of apoptosis in human keratinocytes with the photosensitizer QLT0074 via a direct mitochondrial action. Apoptosis. 2003; 8:269–75. [PubMed: 12766487]
116. Alexis F, Pridgen E, Molnar LK, et al. Factors affecting the clearance and biodistribution of polymeric nanoparticles. Mol Pharm. 2008; 5:505–15. [PubMed: 18672949]
117. Guan M, Ge J, Wu J, et al. Fullerene/photosensitizer nanovesicles as highly efficient and clearable phototheranostics with enhanced tumor accumulation for cancer therapy. Biomaterials. 2016; 103:75–85. [PubMed: 27376559]
118. Shi J, Wang B, Wang L, et al. Fullerene (C60)-based tumor-targeting nanoparticles with “off-on” state for enhanced treatment of cancer. J Control Release. 2016; 235:245–58. [PubMed: 27276066]
119. Du B, Han S, Zhao F, et al. A smart upconversion-based light-triggered polymer for synergetic chemo-photodynamic therapy and dual-modal MR/UCL imaging. Nanomedicine. 2016; 12:2071–80. [PubMed: 27184094]
120. Wang H, Agarwal P, Zhao S, et al. Combined cancer therapy with hyaluronan-decorated fullerene-silica multifunctional nanoparticles to target cancer stem-like cells. Biomaterials. 2016; 97:62–73. [PubMed: 27162075]

121. Li Q, Hong L, Li H, et al. Graphene oxide-fullerene C60 (GO-C60) hybrid for photodynamic and photothermal therapy triggered by near-infrared light. Biosens Bioelectron. 2017; 89:477–82. [PubMed: 27055602]

122. Choi J, Lee SE, Park JS, et al. Gold nanorod-photosensitizer conjugates with glutathione-sensitive linkages for synergistic cancer photodynamic/photothermal therapy. Biotechnol Bioeng. 2018; 115:1340–54. [PubMed: 29288576]

123. Sun Q, You Q, Pang X, et al. A photoresponsive and rod-shape nanocarrier: Single wavelength of light triggered photothermal and photodynamic therapy based on AuNRs-capped & Ce6-doped mesoporous silica nanorods. Biomaterials. 2017; 122:188–200. [PubMed: 28131043]

124. Shi J, Chen Z, Wang L, et al. A tumor-specific cleavable nanosystem of PEG-modified C60@Au hybrid aggregates for radio frequency-controlled release, hyperthermia, photodynamic therapy and X-ray imaging. Acta Biomater. 2016; 29:282–97. [PubMed: 26485168]

125. Hamblin MR. Upconversion in photodynamic therapy: plumbing the depths. Dalton Trans. 2018

126. Liu X, Zheng M, Kong X, et al. Separately doped upconversion-C60 nanoplatform for NIR imaging-guided photodynamic therapy of cancer cells. Chem Commun (Camb). 2013; 49:3224–6. [PubMed: 23482948]

127. Cataldo F, Iglesias-Groth S, Manchado A. On the Molar Extinction Coefficient and Integrated Molar Absorptivity of the Infrared Absorption Spectra of C60 and C70 Fullerenes. Fullerenes, Nanotubes and Carbon Nanostructures. 2011; 20:191–9.

128. Zhang P, Huang H, Huang J, et al. Noncovalent Ruthenium(II) Complexes-Single-Walled Carbon Nanotube Composites for Bimodal Photothermal and Photodynamic Therapy with Near-Infrared Irradiation. ACS Appl Mater Interfaces. 2015; 7:23278–90. [PubMed: 26430876]

129. Huang L, Wang M, Huang YY, et al. Progressive cationic functionalization of chlorin derivatives for antimicrobial photodynamic inactivation and related vancomycin conjugates. Photochem Photobiol Sci. 2018

130. Andreoni A, Nardo L, Bondani M, et al. Time-resolved fluorescence studies of fullerene derivatives. J Phys Chem B. 2013; 117:7203–9. [PubMed: 23646878]

131. Lin S, Jones DX, Mount AS, et al. Fluorescence of Water-Soluble Fullerenes in Biological Systems. NSTI--Nanotech. 2007; 4:238–41.

132. Yu C, Canteenwala T, Chen HH, et al. Hexa(sulfobutyl)fullerene-induced photodynamic effect on tumors in vivo and toxicity study in rats. Proc Electrochem Soc. 1999; 99:234–49.

133. Yin R, Wang M, Huang YY, et al. Photodynamic therapy with decacationic [60]fullerene monoadducts: effect of a light absorbing electron-donor antenna and micellar formulation. Nanomedicine. 2014; 10:795–808. [PubMed: 24333585]

134. Mroz P, Xia Y, Asanuma D, et al. Intraperitoneal photodynamic therapy mediated by a fullerene in a mouse model of abdominal dissemination of colon adenocarcinoma. Nanomedicine: nanotechnology, biology, and medicine. 2011; 7:965–74.

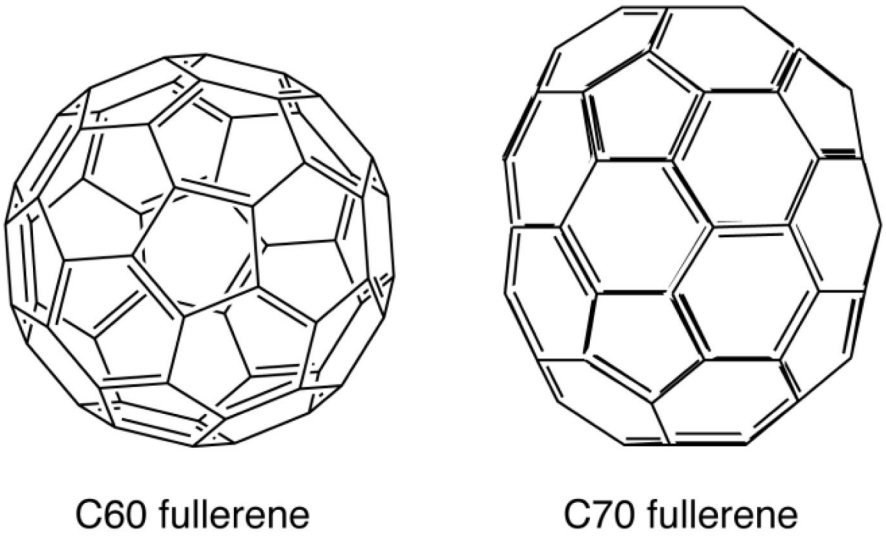

Figure 1.
Structures of C60 and C70 Fullerenes

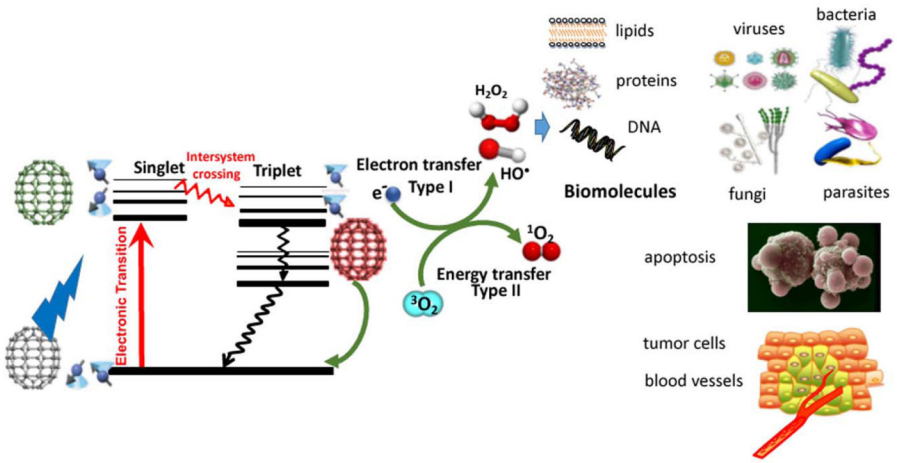

Figure 2. Jablonski diagram

A ground-state fullerene absorbs a photon, transitions to the short-lived (nsec) excited singlet state that can undergo intersystem crossing to the long-lived (μsec) excited triplet state. The triplet fullerene can relax to ground state by emitting phosphorescence, but can also undergo energy transfer with ground state triplet oxygen ($^3O_2$) to form reactive singlet oxygen ($^1O_2$, Type 2) or else can undergo an electron transfer reaction to form HO•, superoxide and H_2O_2 (Type 1). These ROS ($^1O_2$ and HO•) can damage lipids, proteins and nucleic acids leading to destruction of all types of microbial cells, and efficiently kill cancer cells and destroy tumors.

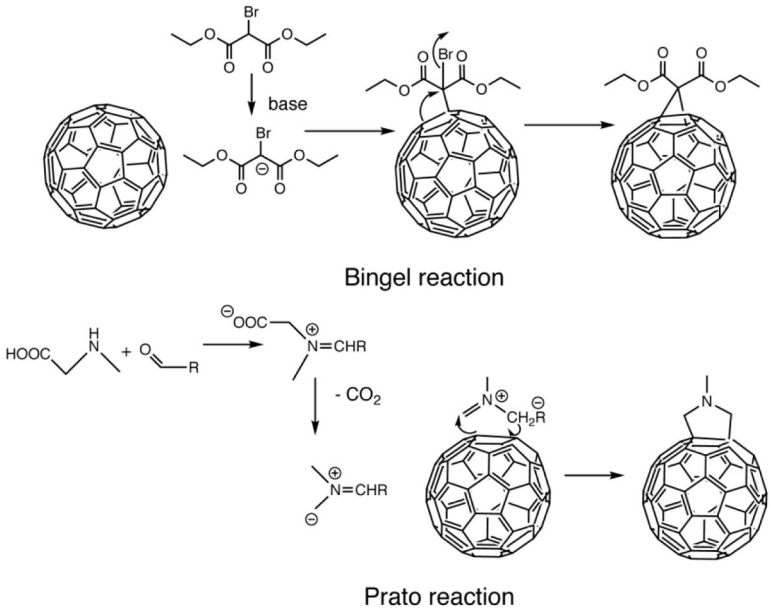

Figure 3.
Mechanisms of the Bingel and Prato reactions for functionalization of fullerenes.

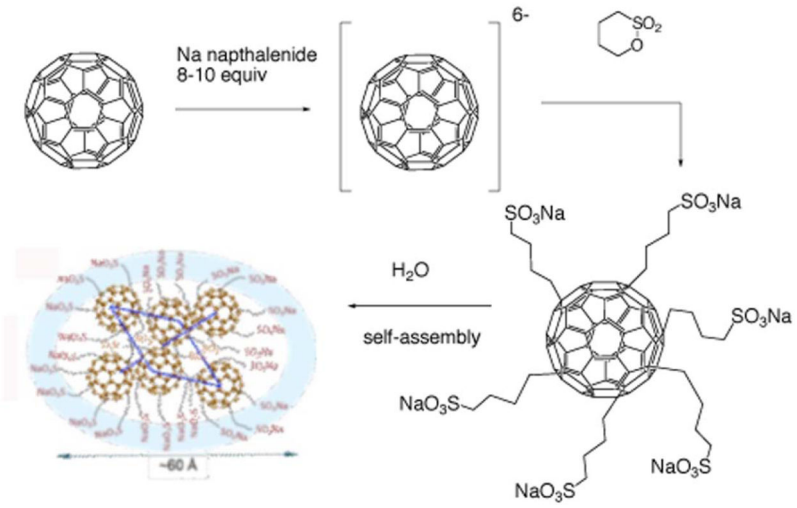

Figure 4.

Synthesis of hexaanionic hexa(sulfo-n-butyl)-C60 (FC4S) and self-assembly into hexameric nanospheres [35, 132].

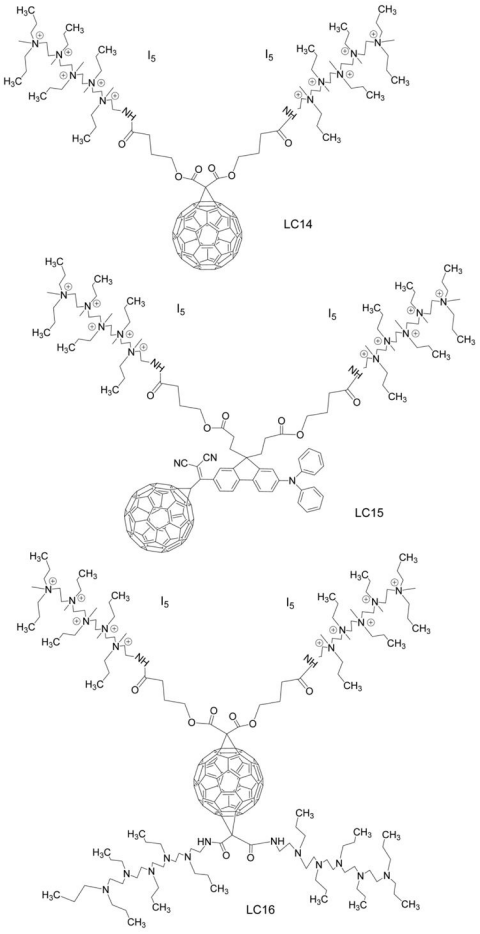

Figure 5. Deca-cationic fullerenes and derivatives LC14, LC15, LC16
Structures of LC14, LC15, LC16 [101, 133]

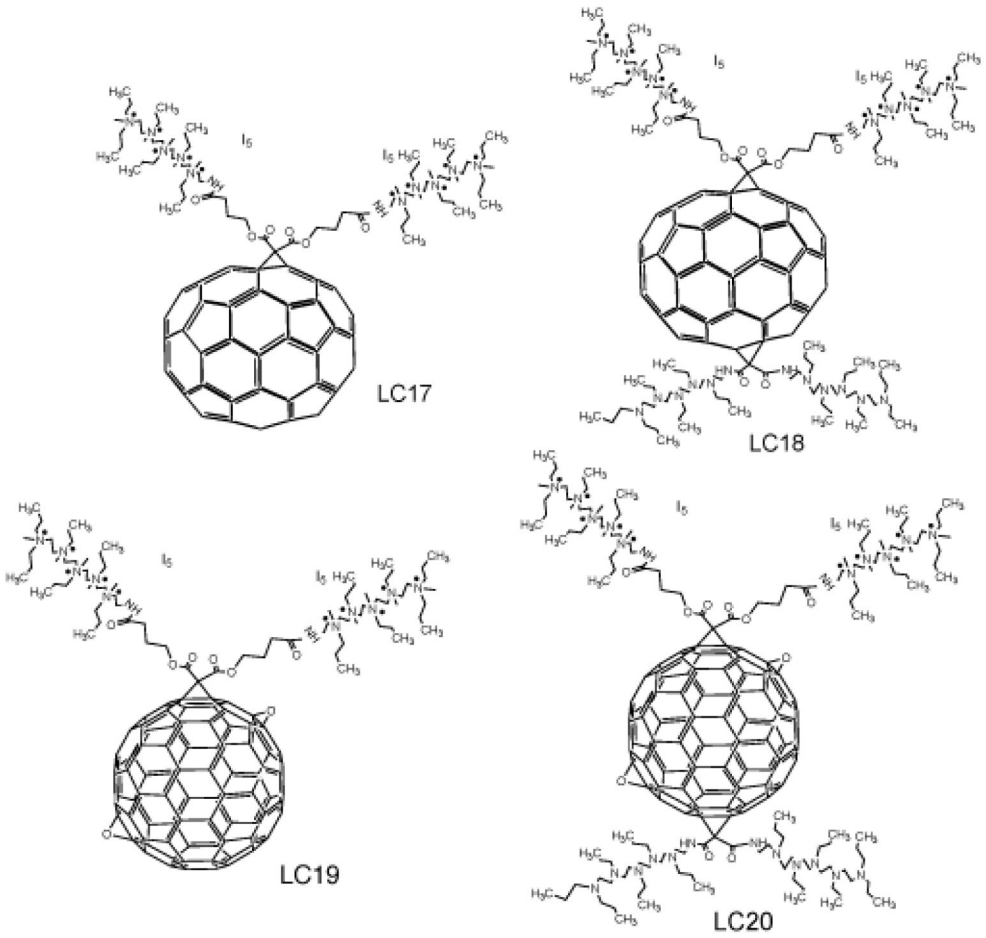

Figure 6. Deca-cationic extended (C70 and C84) fullerenes and derivatives LC 17, LC18, LC19, LC20

Structures of LC17, LC18, LC 19, LC20 [40]

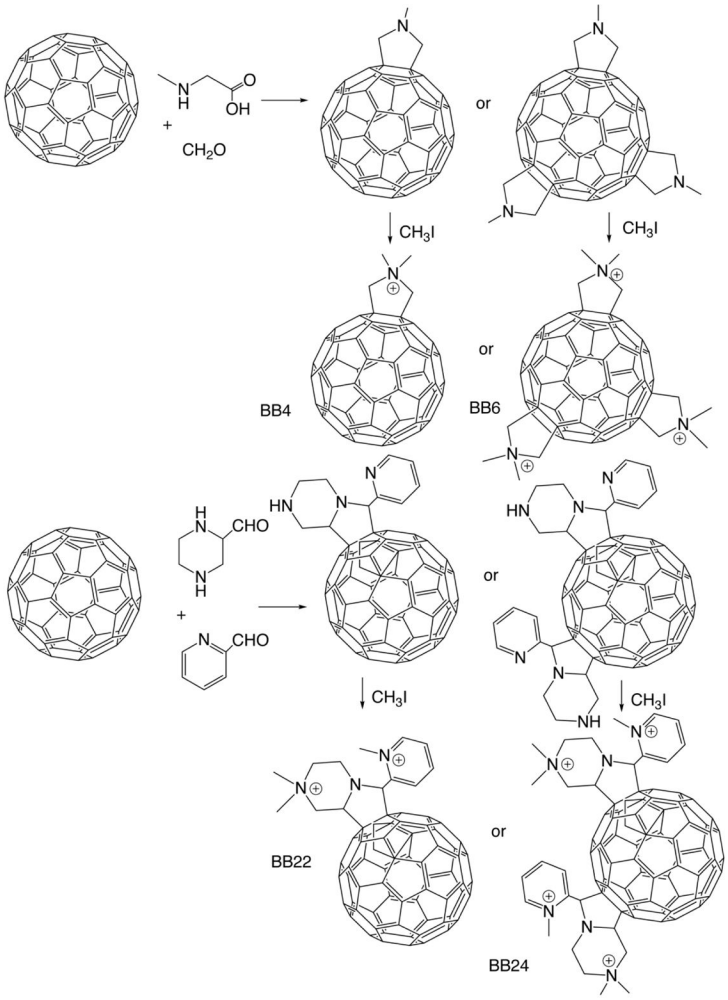

Figure 7. BB4, BB6, BB22, BB24

Synthesis of monocationic and tricationic dimethylpyrrolidinium [60]fullerenes BB4 and BB6 [102], and mono- and bis(piperazinopyrrolidinium) [60]fullerenes BB22 and BB24 [43]

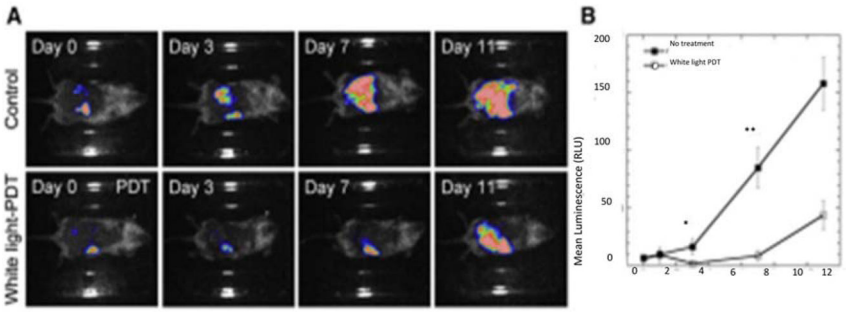

Figure 8. Intraperitoneal PDT of disseminated colon cancer using BB4

(A) Bioluminescence imaging of CT26-Luc tumors growing in a representative control mouse (upper panel) and a representative IPPDT treated mouse (lower panel).

(B) Quantitative analysis of bioluminescence dynamics in control and white light treated mice (n = 10 per group). Reprinted with permission from [134]

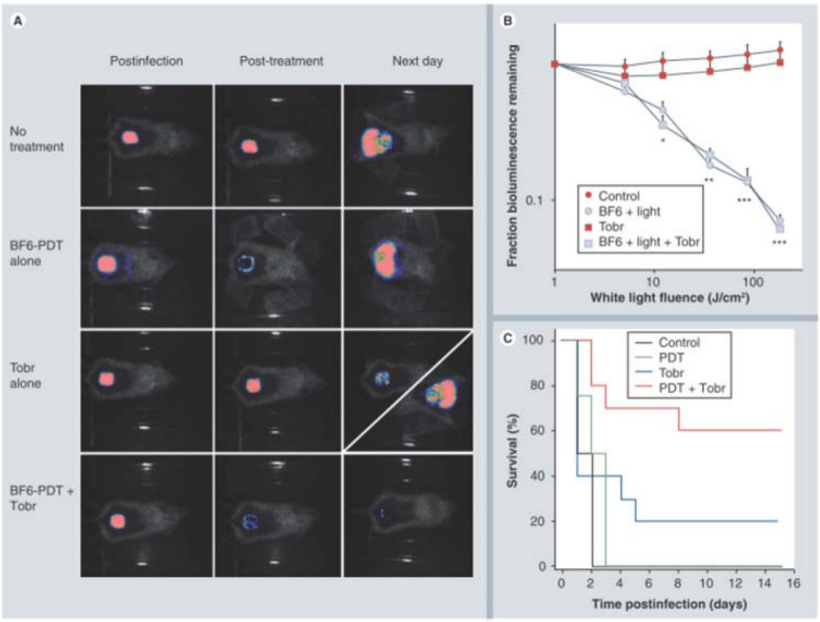

Figure 9. BB6-PDT and tobramycin treatment of *Pseudomonas aeruginosa* wound-infected mice

(A) Representative bioluminescence images of *P. aeruginosa*-infected mice (captured immediately post-infection, immediately post-treatment and 24 h post-treatment), receiving: no treatment (top row); treated with BB6, diagonal panel 24 h post-treatment shows two possible outcomes); and treated with a combination of BB6-PDT and 1 day Tobr (bottom row). (B) Quantification of luminescence values from bioluminescence images (not shown) obtained during the PDT process, or at equivalent times for non-PDT mice. *$p < 0.05$; **$p < 0.01$; ***$p < 0.001$; BB6 plus light (with and without Tobr) versus BB6 in dark and versus Tobr alone. (C) Kaplan–Meier survival curves for the groups of mice in Figure 9A; no treatment control (n = 10); PDT alone (n = 12); Tobr alone (n = 2); PDT plus Tobr (n = 10). PDT: Photodynamic therapy; Tobr: Tobramycin. Reprinted with permission from [42]

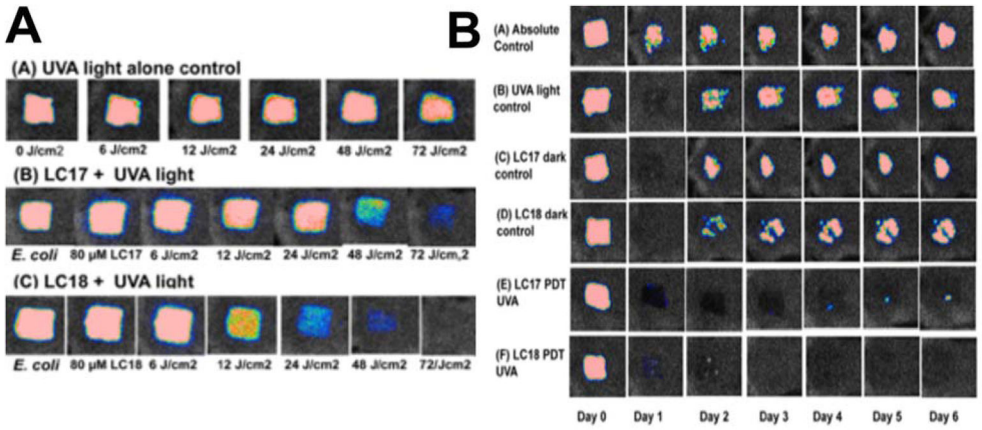

Figure 10. PDT of burn infections with LC17 and LC18

(A) Representative bioluminescence images from mice with *Escherichia coli* burn infections (day 0) and treated with successive fluences of photodynamic therapy or UVA light alone. (A) UVA control; (B) LC17 + UVA light; and (C) LC18 + UVA light. There was no significant reduction in bioluminescence after application of either LC17 or LC18 without light exposure as a dark control. (B). Representative bioluminescence images from mice with *Acinetobacter baumannii* burn infections and treated with PDT, UVA light alone or absolute control, captured day 0 (before photodynamic therapy) and then daily for 6 days. (A) Absolute control; (B) UVA control + 15% DMA; (C) LC17 + 15% DMA; (D) LC18 + 15% DMA; (E) LC17 + 15% DMA + UVA light; and (F) LC18 + 15% DMA + UVA light. Reprinted with permission from [105]